α-Olefins Coordination Polymerization Studies with Single Site Catalysts

Diana Dascalescu

A Thesis

in

The Department

of

Chemistry and Biochemistry

Presented in Partial Fulfillment of the Requirements
for the Degree of Master of Science (Chemistry) at
Concordia University
Montreal, Quebec, Canada

August 2008

Your file Votre référence
ISBN: 978-0-494-45286-8
Our file Notre référence
ISBN: 978-0-494-45286-8

ABSTRACT

α-Olefins Coordination Polymerization Studies with Single Site Catalysts

Diana Dascalescu

Due to their unusual physical properties, perfluorocarbon (PFC) solvents have found applications as immiscible reaction medium when unstable reagents are to be used. We became interested in using a fluorous biphasic system (FBS) for the metallocene-based polymerization of α–olefins. Here we present a study on its potential influences on the coordination polymerization mechanism and physical properties of the polymers synthesized in such conditions.

The first step of our study consisted of the design and set-up of a new polymerization reactor. Using zirconocene dichloride and methylaluminoxane (MAO), as catalytic system, preliminary tests of ethylene polymerization were carried out in order to test the system and assess process stability through the evaluation of ethylene polymerization yields and catalyst efficiency parameters (e.g., activity, turn over number, turn over frequency).

Catalyst efficiency parameters were all correlated, suggesting that the presence of a PFC in the reaction medium had a limited influence on the catalyst efficiency with little impact on the kinetics of the coordination polymerization process. When ethylene – 1-hexene copolymerization reactions were performed in FBS, a negative comonomer effect was observed. Catalyst efficiency parameters calculated for FBS conditions were also affected by the presence of two monomers in the reaction medium.

Differential scanning calorimetry (DSC) was used to evaluate the melting temperature and the crystallinity of the synthesized polymers. The copolymers obtained in FBS were characterized by a relative higher proportion of amorphous structure compared to those synthesized in toluene only. The relative proportion of comonomer incorporated in the copolymers synthesized in FBS increased with increasing the 1-hexene concentrations.

Owing to their great potential, the study of FBS for α-olefin polymerization and copolymerization should be pursued until they find widespread application at the plant scale.

Acknowledgements

I would like to thank to my M.Sc. Supervisor, Dr. Philippe G. Merle, for giving me the opportunity to study and carry out research in his laboratory. With his guidance, I have greatly improved my laboratory skills and became more confident in my abilities as a chemist. My development as a scientist is a direct result of his guidance.

I am deeply indebted to Dr. Yves Gelinas, my Administrative Co-Supervisor. Without his encouragement, guidance and support, especially during these last months, this work would not have been completed.

I am also grateful to Dr. Chris Wilds and Dr. Louis Cuccia, my Advisory Committee members, for their permanent encouragement, helpful recommendations and time.

A special thanks to my colleagues Mirabel Eboka and Svetlana Poponeva. They provided helpful advice and a pleasant working atmosphere. Without Mirabel, weekends and late nights in the laboratory would not have been as enjoyable.

Special thanks to the people in the Department of Chemistry who have helped with my research, especially Ms. Rita Umbrasas for her help with the DSC analyses.

And last but not least, my deepest gratitude goes to my family. To my dear daughter, Stefania Alexandra, sorry for the moments when I could not be around and for moments of lack of patience. My appreciation for you, Florin, is beyond words. I am fortunate to share my life with a person with so much love and patience. I especially appreciate your understanding during the final stages of my work.

Table of Contents

List of Figures

List of Tables

List of Special Symbols

Å	Angstrom
α	alpha
^{0}C	degree Celsius
Cp	cyclopentadienyl (η^5-C_5H_5)
Δ, δ	delta
Et	ethyl
EtOH	ethanol
FBS	fluorous biphasic system
g	gram
ΔG	Gibbs free energy change
GPC	Gel Permeation Chromatography
h	hours
ΔH	enthalpy change
HDPE	high density polyethylene
L	liter
LDPE	low density polyethylene
LLDPE	linear low density polyethylene
M	mole per liter
MAO	methylaluminoxane
MMAO	modified methylaluminoxane
Me	methyl
M	metal
M_n	number average molecular weight
Mw	weight average molecular weight
min	minute
mL	milliliter
NMR	nuclear magnetic resonance
p	pressure

p_{in}	initial pressure
p_{fin}	final pressure
PFC	perfluorocarbons
psi	pound per square inch
π	pi
R	universal gas constant
sc-CO_2	super-critical carbondioxide
ΔS	entropy change
σ	sigma
t	time
T	absolute temperature
T_g	glass transition temperature
T_m	melting temperature
TMA	trimethylaluminium
TOF	turn over frequency
TON	turn over number
v	volume
UHMWPE	ultra high molecular weight polyethylene
Xc	crystallinity percentage
w	weight

Chapter 1 Background and research objectives

1.1 Background

Polyolefins, especially polyethylene and polypropylene, are the most widely used commodity thermoplastic polymers around the world. Compared with thermosets which solidify irreversibly when heated, thermoplastics materials present the advantage that they soften when exposed to heat and then return to their initial condition when cooled. Due to their properties such as strength, flexibility, stability, easy processability and recycling possibilities, thermoplastics represent successful options for more expensive natural and other synthetic materials. They also offer innovative, promising and sustainable approaches for new and unexpected applications.

In 2005 the worldwide polyolefin production was estimated at 110 million tons (70 million tons of polyethylene (PE) and 40 million tons polypropylene (PP)).[1] For 2010, 150 million tons is the estimation for total polyolefins production, an amount which would be sufficient to build 44 Keops Great Pyramids.[2,3] Polyolefins are not new materials – they have been known since 1920 when Herman Staudinger introduced the term "macromolecules" to better describe polymer structure. For his pioneering work in polymer science, Staudinger received the Nobel Prize for Chemistry in 1953. Polyolefins are obtained during a vinyl polymerization by the chain growth addition polymerization of α-olefin monomers (Figure 1.1) during which the double bond is converted into two saturated σ-bonds (Figure 1.2).

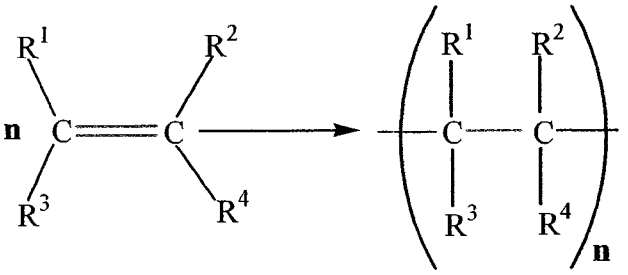

Figure 1.1 Schematic representation of a vinyl polymerization reaction

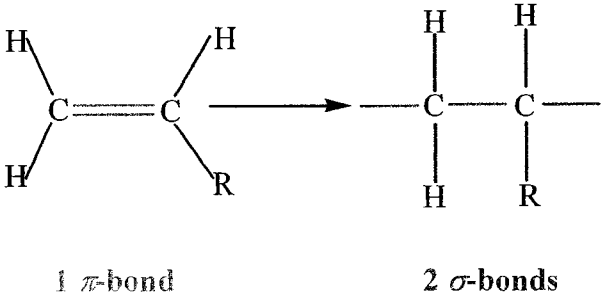

Figure 1.2 Schematic representation of a π-bond conversion into σ-bonds

The compound that contains a carbon-carbon double bond and one hydrocarbon substituent (which can be either a hydrogen, alkyl, aryl, nitrile, ester, acid, ketone, ether or a halogen) is also known as a α-olefin. The resulting polymer, synthesized through a vinyl polymerization reaction, is a polyolefin. The polymer repeating unit contains same number of atoms as the monomer.

This transformation of each π-bond into two σ-bonds makes the vinyl polymerization reaction favorable from a thermodynamic point of view:

$$\Delta G = \Delta H - T\,\Delta S < 0$$

α-olefin polymerization is an exothermic process (e.g. $\Delta H < 0$) due to the conversion of each π-bond from the monomeric unit in two σ-bonds in the polymer repeating unit.

Being a chain growth process, there are three distinct, yet simultaneous steps involved in the reaction: (*i*) initiation – when the reactive species are formed; (*ii*) propagation – which takes place only through the reaction between the monomer and the reactive end-group of the growing chain; and (*iii*) termination - when the reactive centers disappear during specific reactions depending on reactive center type and reaction conditions.

Other characteristics also differentiate a chain growth mechanism from a step polymerization one: (*i*) the monomer is present at any instant in the reaction mixture and its concentration decreases steadily throughout the course of the reaction; (*ii*) the monomer reacts only with the reactive center, by successive additions; (*iii*) the polymer starts to form immediately and, at any instant, the reaction mixture contains only the monomer, the high-molecular weight polymer and the initiator species; (*iv*) the polymeric chain grows fast; (*v*) the polymer molar mass and the reaction yield depend on mechanistic details (e.g., ratio between co-catalyst and pre-catalyst, chain transfer reactions, etc.).

Depending on polymer structure, polyolefins are classified into high density polyethylene (HDPE) with few or no branches on the main polymeric chain, linear low density polyethylene (LLDPE) with many short branches, low density polyethylene (LDPE) with both short and long length branches and ultra high molecular weight polyethylene with no branches on the main polymeric chain.

Looking back on the history of the polymers industry, we can easily notice that the technological development was cyclic with periods of evolution following periods of revolution (Figure 1.3).[4]

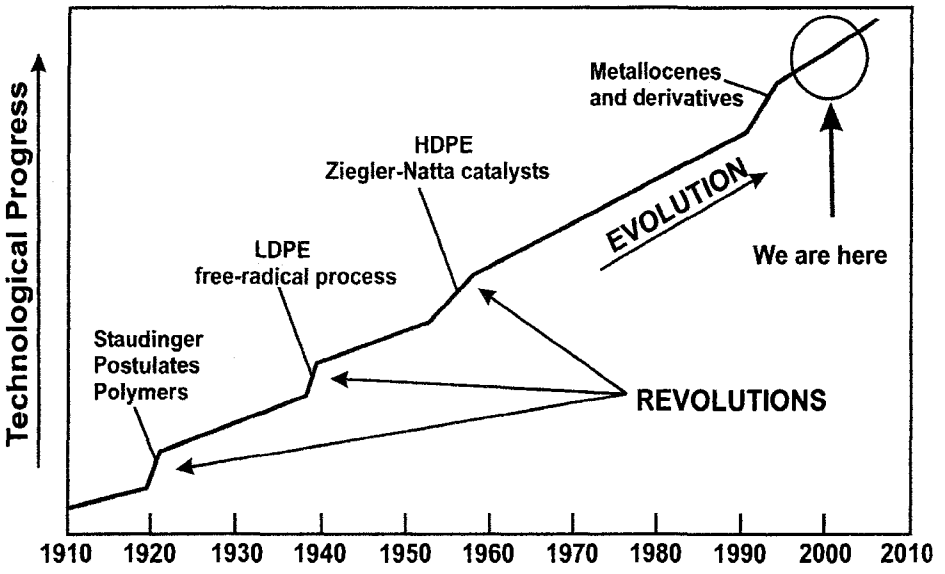

Figure 1.3 Revolution-evolution cycles in the polymer industry

The second revolution took place in the 1940's when low density polyethylene was synthesized for the first time at industrial scale by a free-radical polymerization process. In the 1950's, high density polyethylene was produced using Ziegler-Natta catalysts by a coordination polymerization process. Nowadays the polyolefin technology is developing its fourth revolution represented by the metallocene and other single-site catalysts technologies. The first process that was used at industrial scale to produce polyethylene is free radical polymerization which is carried out at high pressures (e.g., 17,000 – 43,000 psi) and at high temperatures (e.g., 80 – 300 °C). Because of the highly demanding reaction conditions and specific technological characteristics, the set-up for a free radical polymerization reactor is very expensive. Free radical polymerization is a chain growth reaction: the polymer forms through the addition of the monomer to the free-radical active center of the growing chain (Figure 1.4).

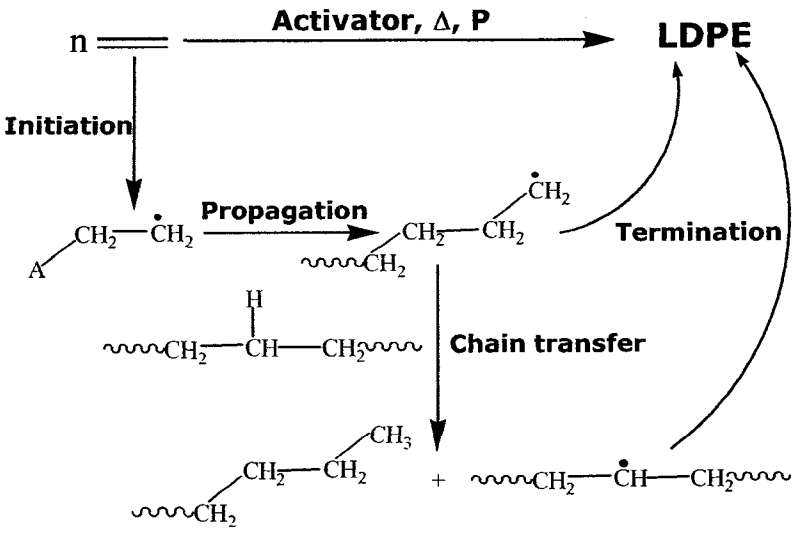

Figure 1.4 Ethylene free-radical polymerization mechanism

In the presence of the initiator, under specific reaction conditions, the active species – the free radicals, form during the initiation step. Propagation involves the growth of the polymer chain by sequential addition of the monomer to the active center. For most monomers, this type of reaction takes place very rapidly with a constant rate of propagation in the range of $10^2 - 10^4$ mol^{-1} s^{-1}.[5] During the termination stage, the growth of polymeric chain stops. Two termination reactions are possible: combination, when two growing chains can combine together; and chain transfer, when the active species is transferred to another component of the reaction mixture (e.g., monomer, initiator, or solvent). The consequence of the intermolecular chain transfer reactions is the formation of a new radical which can reinitiate the polymerization process. That results in the formation of both short and long chain branches on the main polymer chain.

Due to process characteristics, the polymer obtained by a free radical polymerization is also known as the high pressure low density polyethylene (LDPE) and

it is characterized by a high degree of branching and broad molecular weight distribution. The branches that are formed significantly decrease the polymer density and also affect its mechanical properties (e.g., low T_g and crystallinity, excellent processability). As a consequence, LDPE is suitable for the manufacture of thin films, which represent more than 60% of the polyethylene consumption world-wide.

Until the discovery of Ziegler-Natta catalysts, the free radical polymerization process was the only one available to commercially produce significant amounts of polyethylene. In 1953, Karl Ziegler and his group discovered heterogeneous catalysts based on titanium halides ($TiCl_3$) to produce high density polyethylene in the presence of an organoaluminium cocatalyst by coordination polymerization at low pressure and moderate high temperature.[6] This achievement was soon followed by the discovery of Giulio Natta and his coworkers who independently succeeded in the synthesis of isotactic polymers (e.g., polypropylene) using the same organometallic catalytic system.[7] The importance of their work was recognized in 1963 when Ziegler and Natta shared the Nobel Prize for Chemistry for their discoveries in the field of Chemistry and Technology of High Polymers.[8]

The importance of the Zigler-Natta catalyst for the industrial production of polyolefins is remarkable and nowadays several different processes exist using these catalytic systems.[9,10] The most important innovations introduced by Ziegler-Natta catalysts are the synthesis of linear high-density polyethylene (HDPE), ethylene – α-olefins copolymerization to linear low-density polyethylene (LLPE) and the production highly stereoregular polypropylene. The most widely accepted mechanism of polymer chain growth during a coordination polymerization using Ziegler-Natta catalysts is the

one proposed by Cossee and Arlman.[11] A schematic representation of this mechanism is presented in Figure 1.5.

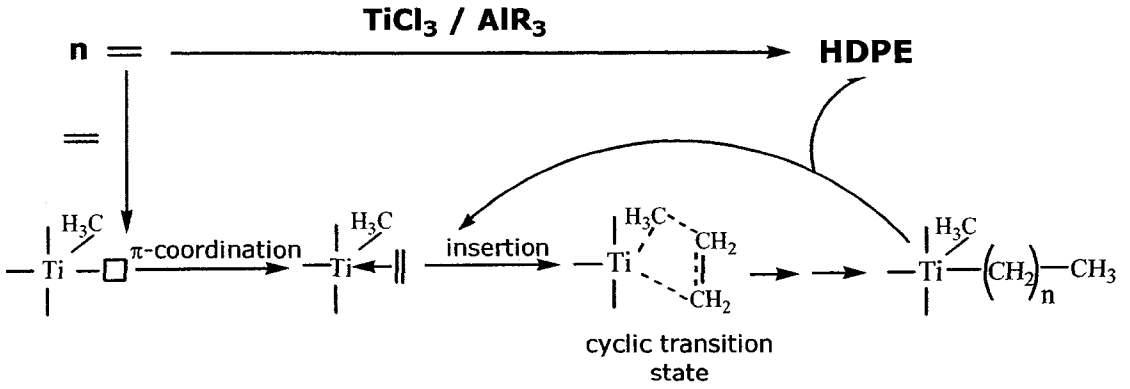

Figure 1.5 General representation of the coordination polymerization using Ziegler-Natta catalysts

Considering the scheme proposed by Cossee and Arlman, the olefin insertion takes place by the coordination of the monomer at the active metal center followed by the *cis*-opening of the double bond. Once the monomer is inserted, a chain migration takes place generating a vacant site where a new monomer molecule can insert which allows the growth of polymeric chain. Due to reaction conditions, both the catalytic system and the resulting polymer are insoluble in the reaction medium. The heterogeneity of the catalytic system determines the presence of many different active sites on the catalyst surface characterized by different catalytic activities and selectivities towards monomer insertion. Even though these systems are characterized by very high activities, the presence of multiple catalytic sites also determines the broad molecular weight distributions and non-uniform comonomer incorporation, thereby influencing the polymer final physical and mechanical properties. Despite these drawbacks, the processes

using heterogeneous Ziegler-Natta catalysts are extensively used and are expected to remain the dominant catalytic route for the production of large volume and low cost polyolefin.[1]

Single-site catalysts like titanocene and zirconocene dichlorides (Cp_2MCl_2, with M = Ti, Zr) were first studied by Breslow and Natta in 1957, which represents the start of the metallocene-based catalyst evolution. The discovery of Kaminsky and his group in 1976 that the methylalumoxane (MAO) can act like a coactivator of zirconocene dichloride represents a new start-up for the polyolefin industry.

In comparison with Ziegler-Natta, the single-site catalysts are soluble in reaction medium and form, at least at the beginning of the process, a homogeneous system. Due to the single-site character of active sites, these catalysts exhibit uniform catalytic activities and allow the synthesis of tailor made polymers with narrow molecular weight distribution and well-defined physical and mechanical properties.

The introduction of single-site catalyst technology at the industrial scale resulted in an impressive rate of innovation of new polymer families at industrial scale. If in the last 55 years only four product families were developed and commercialized, in the next ten years, eleven new polyolefin families are introduced at industrial scale only because of advanced single-site catalysis (Figure 1.6).[4]

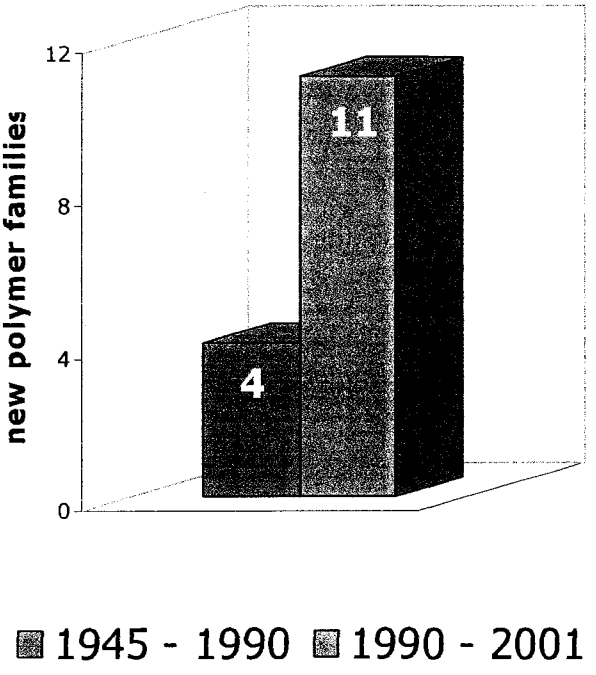

Figure 1.6 Polymer technology revolution determined by single-site catalysis

One examples of a new product developed using single-site catalysis technology is the ultra high molecular weight polyethylene (UHMWPE). Obtained by a coordination polymerization, with molar masses of over 10^6 g mol^{-1} and no branches on the main polymeric chain, UHMWPE is characterized by outstanding physical and mechanical properties such as high abrasion resistance, high impact toughness, good corrosion and chemical resistance, as well as resistance to cyclic fatigue.[12] Due to its excellent properties, UHMWPE is used in highly demanding applications (e.g., artificial implants, and artificial fibers such as Spectra® and Dyneema®).[13]

Nowadays there is a growing interest in developing clean chemical synthesis technologies during which highly efficient chemical reactions produce little or no waste. Alternative pathways proposed by green chemistry approaches ensure that as much of the substrate and reagents as possible find their way into the final product and the use of auxiliary compounds such as solvents and promoters is minimized or even eliminated. In this general context, fluorine chemistry plays an important role in clean technologies, both in catalysts and solvent replacement technologies. Fluorine is a very light element that provides excellent value in terms of activity-per-gram. Due to their specific and unusual properties (e.g., low surface tensions, dielectric constants and refractive indices, high densities, viscosities and gas solubilities), it is also recognized that fluorochemicals are frequently more effective and are required in smaller quantities than non-fluorinated compounds.[14]

Perfluorocarbon (PFC) solvents are saturated aliphatic compounds (e.g., perfluoroalkanes, perfluoroalkyl ethers, perfluoroalkylamines) with unusual properties such as high density, high stability, extremely low solubility in water and organic solvents.[15] Owing to their physical properties, PFC found applications like immiscible reaction medium when unstable reagents are to be used, for heat transfer and for temperature control. J. Rábai and I.T. Horváth introduced the term of "fluorous" and reported the first example of fluorous biphasic catalysis in 1994.[16] Since then, more than 800 papers reported about different approaches and findings related to fluorous chemistry[17], a sign of the importance and attractiveness of this new field of chemistry.[18] Examples of coordination polymerization in PFC are extremely rare[19] in comparison with super-critical CO_2 (*sc*-CO_2), including α-olefin polymerization using the "nickel-

Brookhart catalyst" which offers advantages not only in terms of environmental impacts, but also in terms of polymer properties.[20]

Due to similarities between *sc*-CO_2 and PFC, we became interested in metallocene-based polymerization of α-olefin in FBS and its potential influences on the polymerization mechanism and physical properties of the polymers synthesized in such conditions.

1.2 Research objectives

The main objective of this research was to study the influence of the reaction conditions (e.g., reaction medium) on the kinetics of coordination polymerization during an α-olefin (e.g., ethylene) polymerization and copolymerization with a higher α-olefin (e.g., 1-hexene). Zirconocene dichloride and MAO was used as a catalytic system.

More specifically, the work presented here was focused on:

- the design and the set-up of a new polymerization reactor;
- tests of system stability and process stability during polymerization and copolymerization reactions, respectively;
- testing of a new solvent system (e.g., fluorous biphasic system);
- evaluation of solvent system effects on the polymerization kinetics and mechanism;
- investigation of the physical properties of the polymers obtained in such conditions.

Following the above background and research project objectives (Chapter 1), the second chapter presents the general context and the development of homogenous metallocene catalyzed olefin coordination polymerization with representative examples of the most widely used metallocene precursors and activators. The coordination

polymerization mechanism in the specific case of ethylene is also detailed in that section. In addition, Chapter 2 presents the evolution and the implications of the fluorous biphasic system not only in the green chemistry domain but also in terms of its potential in the case of homogenous metallocene olefin polymerization. The description of the materials and equipment used along with the detailed experimental procedures are included in Chapter 3. In Chapter 4, the specific requirements to design and the set-up of a new polymerization reactor to be used for coordination polymerizations using as catalytic system zirconocene dichloride and MAO are presented along with the improvements performed in order to achieve the system stability and process reproducibility. Chapters 5 details the results obtained when a hydrocarbon (e.g., toluene) was used as reaction medium for ethylene polymerization and ethylene – 1-hexene copolymerization. The results obtained when FBS conditions were used to perform the same tests are discussed in Chapter 6. The last chapter presents a general conclusion of the work accomplished.

Dr. P.G. Merle designed and selected the main parts of the initial reactor set-up. During my project, I assembled the system and worked to improve it in order to achieve the system stability and process reproducibility. I also carried out all the polymerization reactions and characterization analyses described in this thesis.

Chapter 2 Introduction

Key of many other chemical transformations, catalysis also plays a significant role in the controlled synthesis of polymeric materials with predictable and desired properties. The pathways which involve the use of different catalytic systems also have a direct impact on materials performance and gives the opportunity to better respond to the purpose for which the polymers were designed and developed.

2.1 Homogeneous Metallocene Catalyzed Olefin Coordination Polymerization

Metallocenes were the first homogeneous polymerization catalysts reported. In the 1950's, Breslow[21] and Natta[22] made a few attempts to polymerize ethylene using titanocene dichloride (Cp_2TiCl_2) in the presence of aluminum alkyl compounds (e.g., triethylaluminum chloride $AlEt_3$ and diethylaluminum chloride $AlEt_2$), as cocatalysts, such as in classical heterogeneous Ziegler-Natta coordination polymerization catalysis. Even though this catalytic system proved to have low activity/stability and a very low polymer yield, these events mark the beginning of single-site catalyst evolution.[1] Subsequent studies by Long and Breslow[23] led to the idea that the performance of metallocenes activated by alkylaluminum was enhanced when water was added to the system. Adding water to the halogen free Cp_2ZrMe_2 /$AlMe_3$ system, Sinn and Kaminsky[24] observed a high activity for ethylene polymerization and discovered a highly efficient activator, methylaluminoxane (MAO). This represents the beginning of single-site catalyst revolution in polymer chemistry.

Encouraged by this discovery, further studies were initiated, focusing on olefin polymerization in the presence of a Group 4 (Ti, Zr, Hf) metallocene system, particularly

titanocene (Figure 2.1, M = Ti) and zirconocene (Figure 2.1, M = Zr) as catalyst precursor and methylaluminoxane (MAO) as activator.

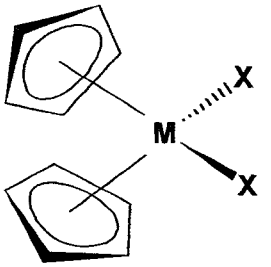

Figure 2.1 Schematic representation of a metallocene (M = Ti, Zr, or Hf).

In comparison with Ziegler-Natta polymerization, single-site catalyst technologies based upon metallocene/activator systems provide a very good control of the polymerization process, in particular of regio- and stereospecificities, molecular weights, molecular weight distributions and comonomer incorporation. All these features enabled the development of new polymeric materials on an industrial scale.

Different studies revealed other specific characteristics of homogeneous single-site metallocene catalysts:

- a large excess of methylaluminoxane (Al/transition metal ratio >500) is required in order to achieve acceptable catalytic activity.[25] Catalyst activity increases with an increasing Al/transition metal ratio.
- a decreased Al/transition metal ratio combined with an increased process temperature results in a lower average polymer molecular weight and, in the case of stereospecific α-olefin polymerization, in decreased stereoregularity.[10]
- catalyst activity decreases in the order Zr > Hf > Ti.[26]

- due to the extremely high activity of catalytically active species (10-100 times higher than that of classical Ziegler – Natta systems)[27], a very low concentration of metallocene is needed in order to obtain effective olefin polymerization (in a range of hundredths of ppm with respect to the monomer). This is the reason for the high sensitivity of these catalysts towards deactivation in the presence of traces amount of water and/or oxygen.
- polymerization rates are very high and the time of chain growth is approximately 10^{-3} – 10^{-2} s. For example, with a degree of polymerization of 10,000, a single act of insertion lasts about 10^{-6} – 10^{-5} s, which corresponds to the duration of a fast biological process.[28]
- compared with the polymers obtained using heterogeneous Ziegler-Natta catalysts which are characterized by a broad molecular weight distribution, polymers synthesized in the presence of single-site catalyst have a narrow molecular weight distribution. The difference is due to the nature of the active centers which are non-uniformly distributed and characterized by different activities in the case of Ziegler-Natta catalysts. Owing to the well defined and controllable structure of metallocene catalysts, a polydispersity (M_w/M_n) of 2 can be predicted by Schulz – Flory statistics[9] for olefin polymerized in such conditions. Such polydispersity value is considered as an indication that only a single site catalyst determines the propagation reaction.

2.2 Metallocene precursor

Compared with the main group metals, transition metals of Groups 4b, 5b and 6b have more orbitals available for interactions and can distribute their valence electrons on *d*-orbitals (e.g., different symmetry), which allows the formation of both σ- and π- bonds with reactive substrates. This ability to accommodate inert spectator ligands along with reactive moities represents the basis of the transition metal-based catalyst design. On the other hand, the character of the metal-carbon bond imparts more attractiveness to the transition metal catalysts. Being more electronegative than any transition metal, the carbon atom in this bond is more susceptible to an electrophilic reaction, and the metal center to a nucleophilic attack. However, the polarity of $M^{\delta+} - C^{\delta-}$ bond can be influenced not only by the type of transition metal and its oxidation state, but also by the properties of ancillary ligands. In addition to the electronic factors mentioned above, the reactivity of the metal center is determined by the steric aspects of all ligands present in the organometallic compound structure. In the case of homogeneous catalysis, the ancillary ligands are not only used to stabilize the metal center, but play also a role in the stability, selectivity and activity of the catalytic system.

Many studies concerning polymerization using metallocene catalysts were and are still focused on the modification of the ancillary ligands. The cyclopendienyl fragment can be easily changed for a wide range of substituents to control the steric and electronic properties of the catalyst precursor. In Figure 2.2, some representative examples of such compounds are exemplified: the substitution of the cyclopentadienyl ligand can be an alkyl substitution, an annulated aryl ring (indenyl), two annulated rings (fluorenyl), two

cyclopentadienyl ligands that can be bridged together by a suitable group and that are known as *ansa*-metallocenes.

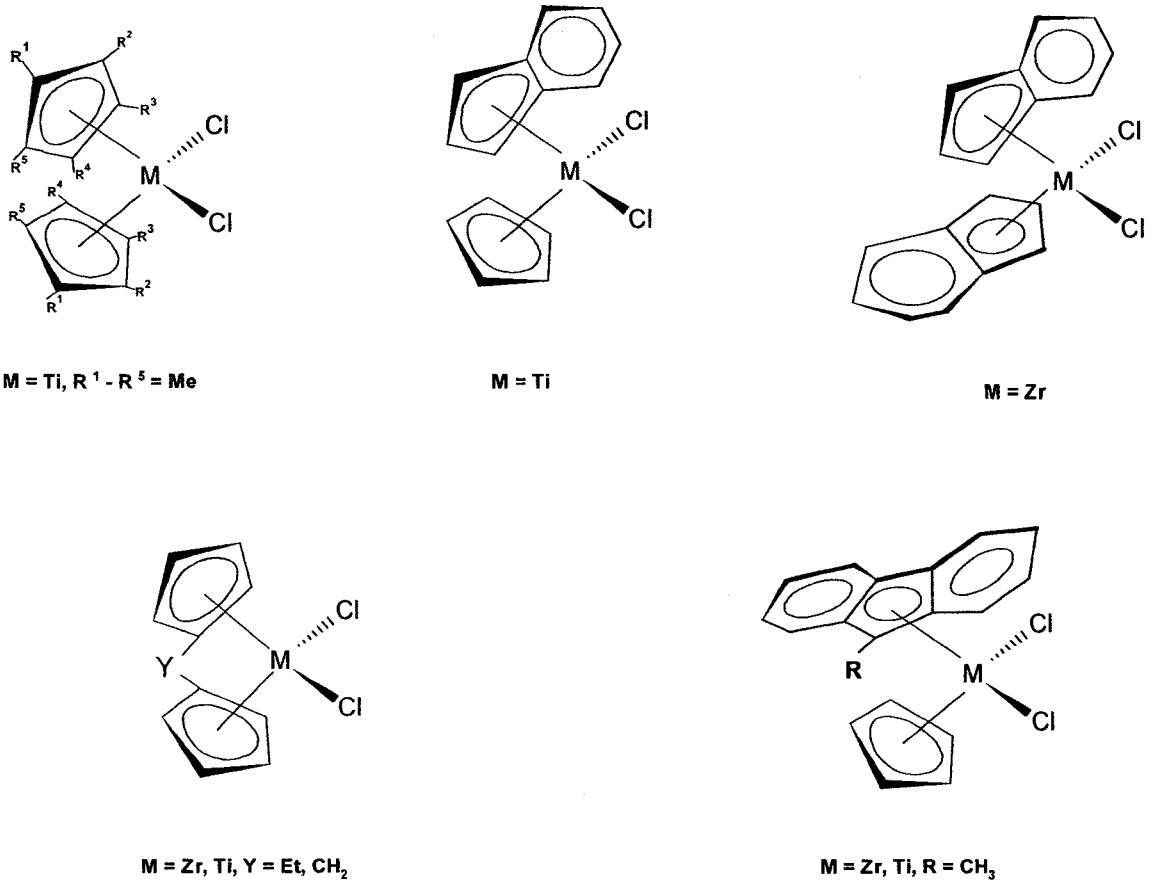

Figure 2.2 Examples of Group 4 metallocene catalysts. Figure adapted from Clemens, Steven N. (2003) Olefin polymerisation using titanium phosphinimide catalysts. M.Sc. dissertation, University of Windsor (Canada), Canada. Retrieved June 24, 2008, from Dissertations & Theses: Full Text database. (Publication No. AAT MR04958).

In the case of a bis-cyclopentadienyl ligand system, each cyclopentadienyl anion donates six electrons to the metal center and the complete delocalization of the electrons in their π-system makes these ligands aromatic, and therefore chemically inert. Such systems where the metal center, particularly an early transition metal, is stabilized by the presence of the cyclopentadienyl ligands has been well studied.

Metallocenes alone cannot however catalyze olefin polymerization as the olefin cannot coordinate to a neutral species. The presence of an activator or cocatalyst is required in order for olefin polymerization reaction to occur.

2.3 Activator

Since Sinn and Kaminsky's discovery, methylaluminoxane (MAO) has become a very important cocatalyst for Group 4 metallocene olefin polymerization. MAO is usually prepared through the controlled hydrolysis of trimethylaluminum (TMA, $AlMe_3$). Even though extensive research has been carried out on the topic in both academia and industry, the exact composition and structure of MAO are not entirely clear or well understood.[29] It is generally accepted that it has an oligomeric structure with typically $n \approx$ 5-20 (Figure 2.3).

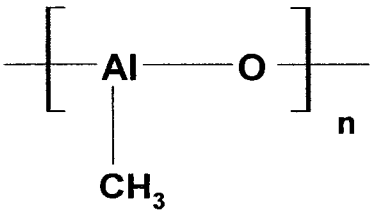

Figure 2.3 A methylaluminoxane functional group

The exact role of the aluminoxane component in olefin coordination polymerization is not known exactly. Through kinetic studies, it has been concluded that besides acting as a scavenger for impurities present in the reaction medium and an alkylation agent, MAO is involved in the formation of a cationic Group 4 metal center with a vacant coordination site (Figure 2.4).[30]

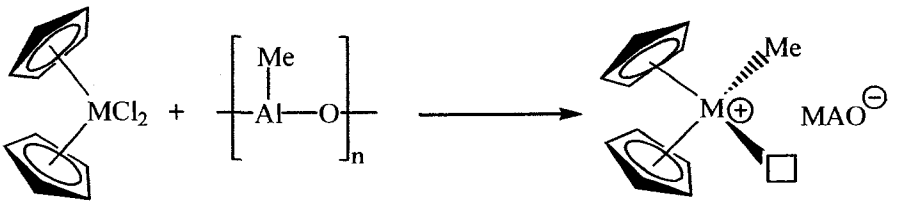

Figure 2.4 Schematic representation of Group 4 metal center with a vacant coordination site formation

Aluminoxanes synthesis is associated with several limitations such as long reaction times to control the reaction exotherm, low yields, risk of explosion and the formation of solid by-products.[31] In order to overcome the drawbacks of the synthesis process along with the ones related with the conventional MAO (e.g., very low solubility in aliphatic solvents, poor storage stability in solution), other aluminoxanes (e.g., ethylaluminoxanes, isobutylaluminoxanes) were synthesized. The modified methylaluminoxanes (MMAO), prepared by controlled hydrolysis of a mixture of trimemethylaluminum and triisobutylaluminum, is characterized by improved solution storage stability in aliphatic solvents and can be produced at lower costs while demonstrating good polymerization efficiency.

While the metallocene catalytic systems in which MAO is used as an activator promoted high to very high activities, they also exhibited a few disadvantages such as the high cost of the cocatalyst since high MAO:catalyst precursor ratios are required (e.g., 10^2 to 10^4:1) for obtaining acceptable polymerization activities. Other matters of concern are related with the poor control over polymer morphology and intrinsically complicated structural features of MAO. As a consequence, new cocatalysts that can provide similar or higher catalytic activity than MAO and that can allow the isolation and separation of the active species in coordination polymerization of olefins were developed. An example is tris(pentafluorophenyl)borane, $B(C_6F_5)_3$, which in early 1990's was studied in combination with Group 4 metallocene by Marks and Ewen for olefin polymerization.[5] In such conditions, highly efficient olefin polymerization was performed and characterizable cationic metallocene complexes were isolated.[5]

2.4 Ethylene Coordination Polymerization Mechanism

Ethylene coordination polymerization, using zirconocene dichloride (Cp_2ZrCl_2) as precatalyst, takes place only in the presence of an activator such as MAO. The formation of the zirconocenium center, which contains a vacant coordination site, takes place during a fast ligand exchange between methyl groups of MAO and chloride in the metallocene catalyst – after methylating Cp_2ZrCl_2, MAO abstracts a methide ligand with active metallocenium polymerization catalyst formation (Figure 2.5).

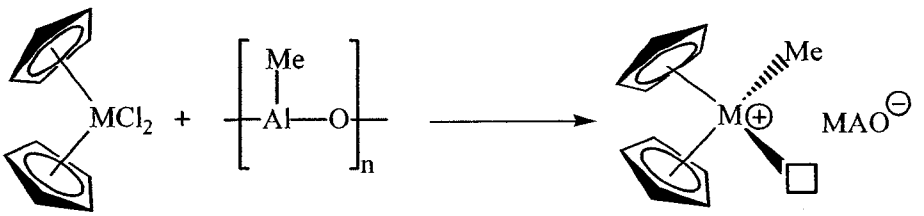

Figure 2.5 Active species formation in the Cp_2ZrCl_2/MAO catalytic system

According to the proposed Cossee-Arlman mechanism[32], in a subsequent step ethylene monomer coordinates to the vacant site of the activated species followed by the insertion into Zr-Me bond through α-agostic hydrogen interaction and rearrangements effects, which help in stabilizing the active species. Chain propagation consists of the insertion of subsequent coordinated ethylene into Zr-polymer σ-bond (Figure 2.6) with the regeneration of a metal-carbon bond.

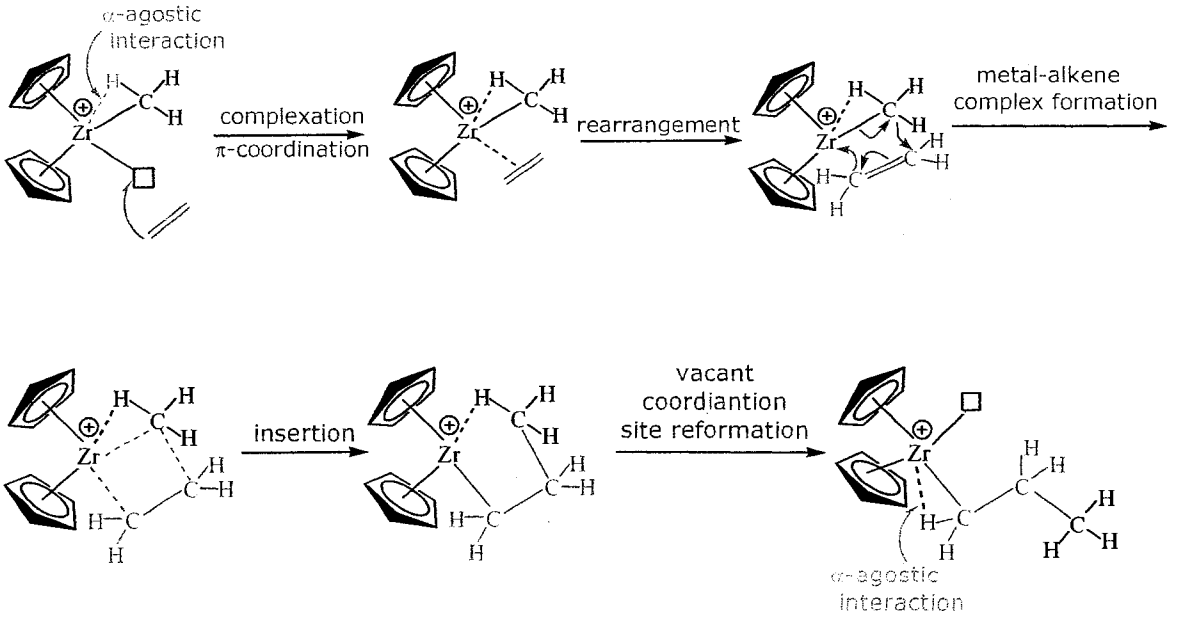

Figure 2.6 Propagation step in ethylene coordination polymerization using Cp_2ZrCl_2/MAO like catalytic system

When no specific chain transfer agent has been added to the polymerization system, three chain transfer reactions are usually considered for the termination step: transfer to monomer (Figure 2.7a), spontaneous transfer (Figure 2.7b) and transfer to the activator (Figure 2.7c). The resultant Zr(IV) products can also insert ethylene into their metal alkyl and hydride bonds with the possibility of new polymeric chains to grow.

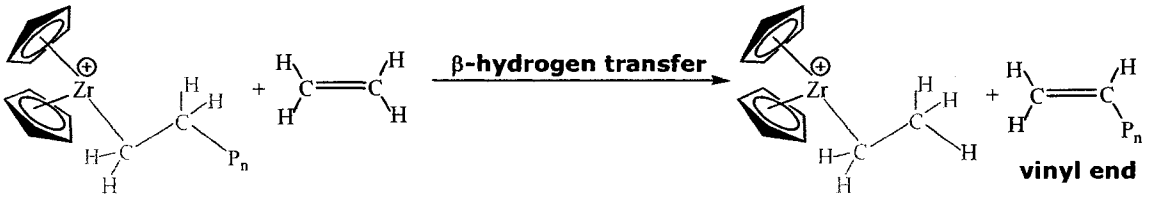

a)

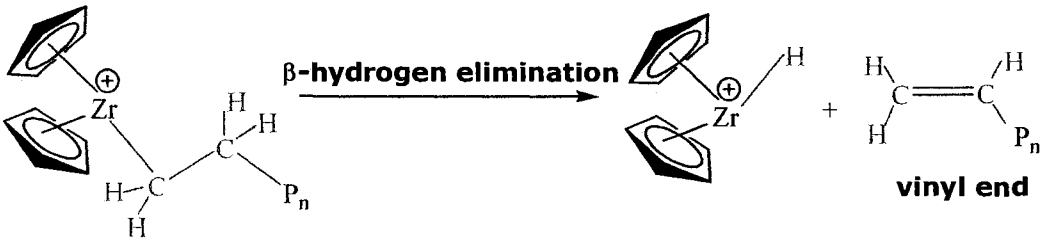

b)

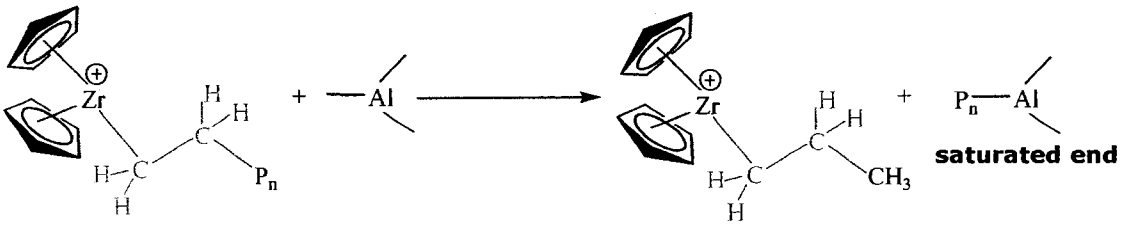

c)

Figure 2.7 Termination step during ethylene coordination polymerization using Cp_2ZrCl_2/MAO like catalytic system: a) chain transfer to monomer, b) spontaneous transfer, c) chain to transfer to activator.

2.5 Copolymerization

The chemically well defined yet easy to be modified structure of metallocene catalysts allows for the possibility to synthesize polymers which, in addition to the main monomeric unit, can incorporate different amounts of a second monomer unit known as comonomer. The final properties of such polymer are definitively marked by the degree of incorporation and the type of comonomer used during the synthesis reaction. The mechanistic features of the copolymerization reaction are in principle similar to those of the homopolymerization. For example, the copolymerization of ethylene with small amounts (< 5%) of higher α-olefins (C_4 – C_{20}) yields a linear polymer with desirable processable properties which are also known as low linear density polyethylene.

2.6 Fluorous Biphasic Solvent System

Based on their physical properties (e.g., low polarity, low dielectric constant, high gas solubility, low evaporation heat), perfluorocarbon (PFC) solvents have been exploited in several applications as an immiscible reaction medium when unstable reagents are to be used, for heat transfer and/or for temperature control. Studies initiated by Horváth and Rábai[33] on the use of the fluorous biphasic concept for catalyst recovery in fluorous biphasic solvent system (FBS) opened new possibilities for the investigation of homogeneous polymerization of olefins in non-conventional reaction conditions.

Few coordination polymerization studies in PFC have been carried out[21] in comparison to *sc*-CO_2, including α-olefin polymerization using the nickel-Brookhart catalyst. This catalyst offers several advantages not only in terms of environmental benefits, but also in terms of polymer properties.[22] Due to similarities between *sc*-CO_2

and PFC, we became interested in metallocene-based polymerization of α-olefin in FBS and its potential influence on the coordination polymerization mechanism and physical properties of the polymers synthesized in such conditions.

A good understanding of chemical processes can be achieved by studying the kinetics of a reaction, which represents a key factor in the adaptation of a process to the industrial scale. Compared to a heterogeneous system, a kinetic study of a homogeneous process is easier to carry out owing to the homogenous character of the different species involved at least at the beginning of the process. It is still however not a simple thing to do. The complexity of a kinetic study in the case of homogeneous polymerization process is due to the reactants precatalyst/cocatalyst system which via a set of specific interactions induces the formation of active species and monomers, α-olefins, and to the reaction product, the polyolefin. Another set of variables is related to the experimental conditions that are used, such as precatalyst and cocatalyst concentration, precatalyst / cocatalyst ratio, type of solvent, reactor vessel design, temperature, pressure, or reaction time (Figure 2.8).

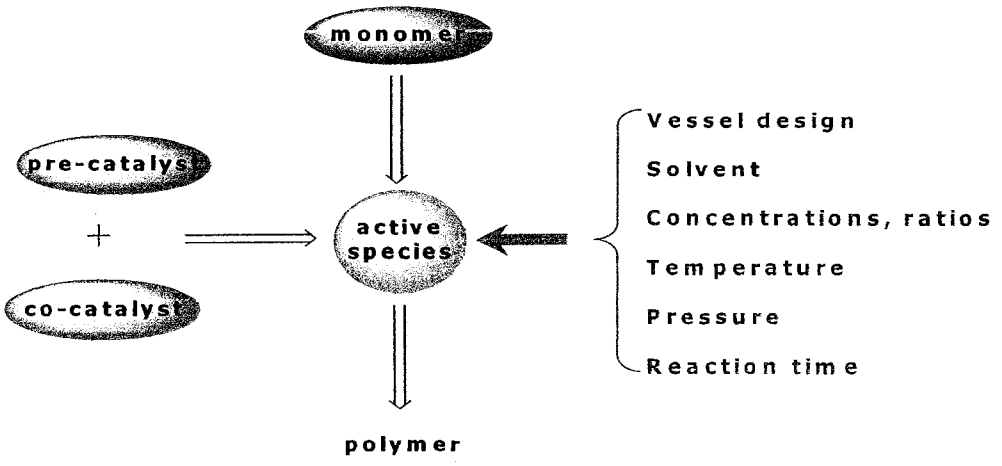

Figure 2.8 Schematic representation of variables to be considered for a kinetic study of homogeneous olefin polymerization

As part of our study, in order to minimize part of the potential errors induced by the presence of such variables, some simplifications were performed: first, Cp_2ZrCl_2/MAO, a very well studied and understood catalytic system, was chosen as the single-site catalytic system; then, ethylene, the simplest α-olefin, and 1-hexene were chosen as the monomeric units. Because of these simplifications, we were able to focus our kinetic study only on the influence of the reaction medium (FBS and PFC) on the α-olefin coordination polymerization and copolymerization.

Chapter 3 Experimental

3.1 Materials

All the experiments were carried out under argon (ultra high purity, 5.0, Praxair) using standard Schlenk techniques. Toluene (certified A.C.S., Fisher Scientific) and 1-hexene (97%, Aldrich), were dried over molecular sieves. Fluorinert electronic liquid FC-72 (3M) was dried over molecular sieves and degassed under argon. Methylaluminoxane, PMAO-IP, (in toluene, 13% wt Al, Akzo-Nobel Polymer Chemicals LLC) was used as received. Al/Zr = 1000. Bis(cyclopentadienyl) zirconium (IV) dichloride Cp_2ZrCl_2, (≥98%, Aldrich) was used as received.

3.2 Equipment

The polymerization tests were performed in a 300-mL reactor (Parr Instrument Co.). The reactor was designed to perform polymerization tests under a wide range of pressures and temperatures. The reactor vessels were either a glass vessel for low pressure working conditions (up to 150 psi) or a stainless steel one designed for high working pressure (up to 1000 psi) at 225 °C. Both reactor vessels were jacketed to allow external cooling/heating in order to allow tests at various temperatures. A supplementary high capacity PC-controlled external cooling/heating circulator (Julabo F32-EH) was used for the better control of the polymerization temperature. For the internal cooling, an internal loop was connected to a second external circulating bath (Fisher Scientific Isotemp 3016) in order to minimize the polymerization exotherm (the amount of heat released at the beginning of the reaction). A PC-controlled solenoid valve allowed the

flow of the cooling fluid though the loop when the reactor internal thermocouple required it.

The gas burette used in this work was a one liter cylinder connected to a pressure transducer. Monitoring the pressure drop gave information about the amount of monomer consumed during a test and about the reaction kinetics. The stirrer was a gas entrainment impeller which minimized the mass transfer limitations. The vacuum created at the tip of the impeller forced the gas into the openings of the shaft and pulled it through the dispersion ports located at the tips of the impeller. The role of the magnetic coupling to the external motor was to eliminate any potential leak. The stirring speed was adjusted and controlled by the Digital RPM Display Module. Two in/out gas/liquid filling ports were used as connections to feed the reactor with the reagents and to ensure suitable reaction conditions.

To ensure an efficient and safe reactor operation mode the reactor set-up was completed with a controller which allowed the full control and tuning of the reaction parameters (e.g., monomer pressure, working temperature, stirring rate) and a data logger which by the mean of suitable software allowed reaction data analysis.

3.3 Polymerization procedure

In a typical polymerization experiment, the reactor was heated for two and a half hours under vacuum, at 80 °C in order to remove traces of water and oxygen. Toluene (45 mL) was transfered to the reactor, followed by the methylaluminoxane (MAO) solution (at 5.5×10^{-2} mol L^{-1}, which is the required amount to achieve an Al:Zr ratio of 1000:1) and then by another portion of toluene (50 mL). The Cp_2ZrCl_2 toluene solution (7.7×10^{-3} mol L^{-1}, which is the required amount for a 5.5×10^{-5} mol L^{-1} of Zr in the

reactor) was then transferred to the reactor, followed by the last portion of toluene (50 mL).

The system was purged three times with argon and then the ethylene was allowed in the system (at t_0), at a constant pressure. At the end of the polymerization time (t_f), the ethylene admission was stopped, the reactor depressurized and the reaction was quenched with a 1:1 mixture EtOH – HCl 2 mol L^{-1} (50 mL). The suspension was filtered and the solid was first rinsed with a 10% HCl (50 mL), then with EtOH (70 mL) and dried, at room temperature until constant mass.

When a copolymerization and/or a test in FBS conditions were performed, the comonomer and/or the perfluorinated solvent were injected before the ethylene monomer was admitted in the system.

3.4 Process reproducibility

A preliminary series of experiments were performed in order to test the system stability and process reproducibility. The yields calculated for each run of the preliminary tests are presented in Table 3.1.

Table 3.1 Reproducibility tests

Run	(p_{in} - p_{fin}) (psi)	Mass C_2H_4 used (g)	Polymer mass (g)	Yield (%)
76	46.0	3.59	4.42	(~100.0)
77	23.0	1.80	2.76	(~100.0)
78	30.0	2.34	4.01	(~100.0)
79	31.0	2.41	3.44	(~100.0)
82	42.0	3.28	3.30	(~100.0)
87	66.0	5.15	6.90	(~100.0)
88	61.0	4.77	5.02	(~100.0)
90	31.0	2.43	2.48	(~100.0)
95	38.0	2.97	4.33	(~100.0)

The experimental conditions used for the preliminary tests were: [Zr] = 5.5×10^{-4} mol L^{-1}, Al/Zr = 500, T_{pol} = 45 °C, monomer pressure $p_{C_2H_4}$ = 2.2 bar, duration = 10 min, solvent: toluene (150 mL). The presence of residual oxygen, water and other impurities in the feed or in the reactor, a poor temperature control during the process and/or irreproducible addition of the catalytic system can explain the inconsistency of the yields obtained during the preliminary tests for process reproducibility (which also explain why the run numbers in Table 3.1 and others are not consecutive - some runs simply did not yield usable data and thus were not considered in this work).

In order to reach stability in our system, a few modifications were done: (*i*) the reactor was pre-treated under vacuum and high temperature (e.g., 80 °C) for two hours; (*ii*) the system was purged three times with argon before monomer introduction; and (*iii*) a supplementary cooling bath was connected to the reactor cooling loop in order to minimize the reaction exotherm.

In parallel, some changes in the experimental protocol were applied: (*i*) stock solutions of pre-catalyst and co-catalyst were prepared in order to reduce the errors associated with the preparation and manipulation of small solution volumes; and (*ii*) the order of addition of the reactants was modified in order to ensure an effective transfer of the small volumes of the reagents and to avoid the deactivation of catalytic active species. Using this improved experimental procedure, the process reproducibility was tested again. The results of these series of tests are presented in Table 3.2.

Table 3.2. Ethylene polymerization yields in toluene

Run	(p_{in} - p_{fin}) (psi)	Mass C_2H_4 used (g)	Actual polymer mass (g)	Yield (%)
159	134.0	10.47	9.29	88.7
160	104.0	8.13	7.16	88.0
161	109.0	8.54	7.42	86.9
166	116.0	9.10	7.77	85.4
167	98.0	7.67	6.72	87.6
172	114.0	8.91	7.73	86.8
173	134.0	10.46	9.66	92.3

Polymerization conditions: [Zr] = 5.5×10^{-4} mol L^{-1}, Al/Zr = 500, T_{pol} = 45 °C, monomer pressure p_{C2H4} = 2.2 bar, duration = 10 min, toluene (150 mL).

The influence of the polymerization time over the polymerization yield and catalysts parameters was also studied. The results of these experiments are presented in Table 3.3.

Table 3.3 Effect of polymerization duration on the polymerization yield

Run	Polymerization time (min)	(p_{in} - p_{fin}) (psi)	Mass C_2H_4 used (g)	Actual polymer mass (g)	Yield (%)
175	40	194.0	15.18	12.07	79.5
162	30	168.0	13.15	10.34	78.6
174	20	132.0	10.35	8.65	83.6
176	1	43.0	3.35	3.87	(~100.0)

Polymerization conditions: [Zr] = 5.5×10^{-4} mol L^{-1}, Al/Zr = 500, T_{pol} = 45 °C, monomer pressure p_{C2H4} = 2.2 bar, duration = 10 min, toluene (150 mL)

The effect of polymerization temperature on the catalyst efficiency parameters was also studied. The results of these tests are presented in Table 3.4.

Table 3.4 Effect of polymerization temperature on the polymerization yield

Run	Polymerization temperature (°C)	(p_{in} - p_{fin}) (psi)	Mass C_2H_4 used (g)	Actual polymer mass (g)	Yield (%)
210		66.0	5.18	5.68	(~100.0)
212	70	80.0	6.25	5.30	84.8
213		69.0	5.38	3.93	73.0
207		93.0	7.28	6.90	94.8
208	60	79.0	6.17	5.45	88.4
209		91.0	7.10	7.04	99.2
214		91.0	7.04	5.91	84.0
215	30	114.0	8.87	8.90	(~100.0)
216		112.0	8.71	8.98	(~100.0)
217	20	97.0	7.53	7.54	(~100.0)

Polymerization conditions: [Zr] = 5.5×10^{-5} mol L^{-1}, Al/Zr = 1000, monomer pressure = 2.2 bar, duration = 10 min, toluene (150 mL)

3.5 Ethylene – 1–hexene copolymerization in toluene

A series of copolymerization tests were run using 1-hexene. The tests were run at different 1-hexene concentrations (0.2, 0.5 and 0.8 mol L^{-1}) for two different polymerization durations (10 minutes and 30 minutes) using the experimental procedure above mentioned. The yield of these tests is presented in Table 3.5.

Table 3.5 Ethylene – 1-hexene copolymerization yields

Run	$[C_6H_{12}]$ mol L^{-1}	Mass C_2H_4 used (g)	Mass C_6H_{12} used (g)	Theoretical polymer mass (g)	Actual polymer mass (g)	Yield (%)	Polymerization time (min)
132	0.2	7.04	2.80	9.84	8.40	85.3	10
131		4.93		7.73	5.40	69.8	30
119	0.50	5.55	6.30	11.85	5.12	43.2	10
129		3.43		9.73	2.74	28.1	
130		3.68		9.98	2.94	29.5	30
121	0.8	2.73	10.08	12.81	1.86	14.5	10
122		3.05		13.13	3.05	23.2	
123		3.52		13.6	3.16	23.2	
128		2.97		13.05	2.50	19.2	
126		4.46		14.54	3.22	22.1	30

Polymerization conditions: [Zr] = 5.5×10^{-5} mol L^{-1}, Al/Zr = 1000, T = 45 °C, monomer pressure = 2.2 bar, duration = 10 min, toluene (150 mL).

3.6 Ethylene polymerization in FBS conditions

During the next step of the project, the effect of fluorous biphasic conditions (FBS) on the ethylene polymerization was studied. The results of these tests are presented in Table 3.6.

Table 3.6 Ethylene polymerization yields in FBS conditions

Run	(p_{in} - p_{fin}) (psi)	Mass C_2H_4 used (g)	Actual polymer mass (g)	Yield (%)
178	93.0	7.28	7.22	99.2
179	99.0	7.73	7.72	99.9
198	106.6	8.34	8.32	99.8
202	107.1	8.36	8.29	99.2
203	87.0	6.78	6.76	99.7

Polymerization conditions: [Zr] = 5.5×10^{-5} mol L^{-1}, Al/Zr = 1000, T = 45 °C, monomer pressure = 2.2 bar, duration = 10 min, toluene:FC 72 = 4:1(v/v), (150 mL).

3.7 Ehtylene – 1-hexene copolymerization in FBS conditions

The effect of fluorous biphasic conditions (FBS) over the ethylene – 1-hexene copolymerization polymerization was also studied. The results of these tests are presented in Table 3.7.

Table 3.7 Ethylene – 1-hexene copolymerization yields in FBS conditions

Run	$[C_6H_{12}]$ mol L^{-1}	Mass C_2H_4 used (g)	Mass C_6H_{12} used (g)	Theoretical polymer mass (g)	Actual polymer mass (g)	Yield (%)
239	0.2	11.07	2.82	13.89	13.86	99.8
242		10.90	2.82	13.72	13.40	97.7
238	0.5	15.45	6.30	21.75	19.80	91.0
204	0.8	7.65	10.08	17.73	8.02	45.2
206		8.17	10.08	18.25	8.22	45.0
237		12.79	10.08	22.87	15.53	67.9

Polymerization conditions: [Zr] = 5.5×10^{-5} mol l^{-1}, Al/Zr = 1000, T = 45 °C, monomer pressure = 2.2 bar, duration = 10 min, toluene:FC 72 = 4:1(v/v), (150 mL), new MAO batch

3.8 Polymer characterization

DSC measurements

The polymer melting points, glass transition temperatures and the crystallinity were measured using a Mettler Toledo FP900 equipped with a FP85 DTA/DSC measuring cell. The samples were heated to 180 °C at a rate of 10 °C min^{-1}, and then cooled to 25 °C in order to remove the thermal sample history. The second DSC scan was recorded using the same heating program. Crystallinity was calculated using the equation $X_c = \Delta H_f / \Delta H_f^\circ \times 100$, where X_c represents crystallinity percentage of the analyzed

sample (%), ΔH_f represents the heat of fusion of the sample, $\Delta H_f°$ represents the heat of fusion for perfect crystalline polyethylene, $\Delta H_f° = 291.7$ J g^{-1}. [45]

FT-IR analysis

Ethylene – 1-hexene copolymers compositions were measured by the IR method following a procedure taken from the literature[34], using a Nicolet 6700 FT-IR (Thermo Electron Corporation). Air was used as the background. Copolymer compositions (Tables 3.8 and 3.9) were measured using the A_{1380}/A_{722} absorbance ratios from the calibration curves for copolymer composition measurement by the FT-IR method described in reference 34.

Table 3.8 Comonomer content in ethylene – 1-hexene copolymers in toluene

Run	$[C_6H_{12}]$ mol L^{-1}	A_{1380} (cm^{-1})	A_{722} (cm^{-1})	A_{1380}/A_{722}	Hexene content, c_{hexene} (%)
132	0.2	0.443	1.179	0.38	8.1
131		0.105	1.515	0.07	1.7
119	0.5	0.052	0.106	0.49	9.9
129		0.700	2.436	0.29	6.8
130		1.015	2.921	0.35	7.5
121	0.8	1.298	0.577	0.44	9.3
122		0.237	0.777	0.31	6.9
123		1.352	1.344	1.01	-
128		1.161	2.053	0.57	9.5
126		0.158	0.134	1.18	-

Table 3.9 Comonomer content in ethylene – 1-hexene copolymers in FBS conditions

Run	$[C_6H_{12}]$ mol L^{-1}	A_{1380} (cm^{-1})	A_{1370} (cm^{-1})	A_{1380}/A_{1370}	Hexene content, c_{hexene} (%)
244	0.2	0.385	0.595	0.65	1.6
245	0.5	0.441	0.529	0.83	3.0
246	0.8	0.724	1.049	0.69	2.7

Chapter 4 Reactor design, set-up and system stability

The metallocene-based ethylene market demand represents only a small percentage of the entire amount of polyethylene produced worldwide. However, analysts forecast a 30 % annual growth from 1 million tons in 2000 to 17 million tons in 2010, based on the advantages and superior material properties of the metallocene-produced polyethylene. By the end of the decade, metallocene-based polyethylene is expected to represent more than one-fifth of the total polyethylene market.[35] For a laboratory process to be successfully transferred to the industrial scale, a key factor is a detailed and complete understanding of the mechanism and the kinetics of the polymerization mechanisms.

Kinetic and mechanistic studies of homogeneous polymerizations with metallocene catalysts are relatively easier than for heterogeneous systems. This is partly due to the well defined characteristics of the single-site catalysts. The starting point for mechanistic and kinetic studies is the design and set-up of a polymerization reactor. This reactor has to fulfill some basic requirements such as the continuous feed of the reagents and monomer and its resistance to severe reaction conditions (high pressure and temperature). Although some mechanistic and kinetic studies of olefins coordination polymerization with related Cp_2ZrCl_2/MAO catalytic systems exist,[36] there are just few published examples for a coordination polymerization reactor design and set-up.[37]

We designed our own reactor to perform polymerization under a wide range of temperatures and pressures. A schematic representation of our reactor set-up is presented in Figure 4.1.

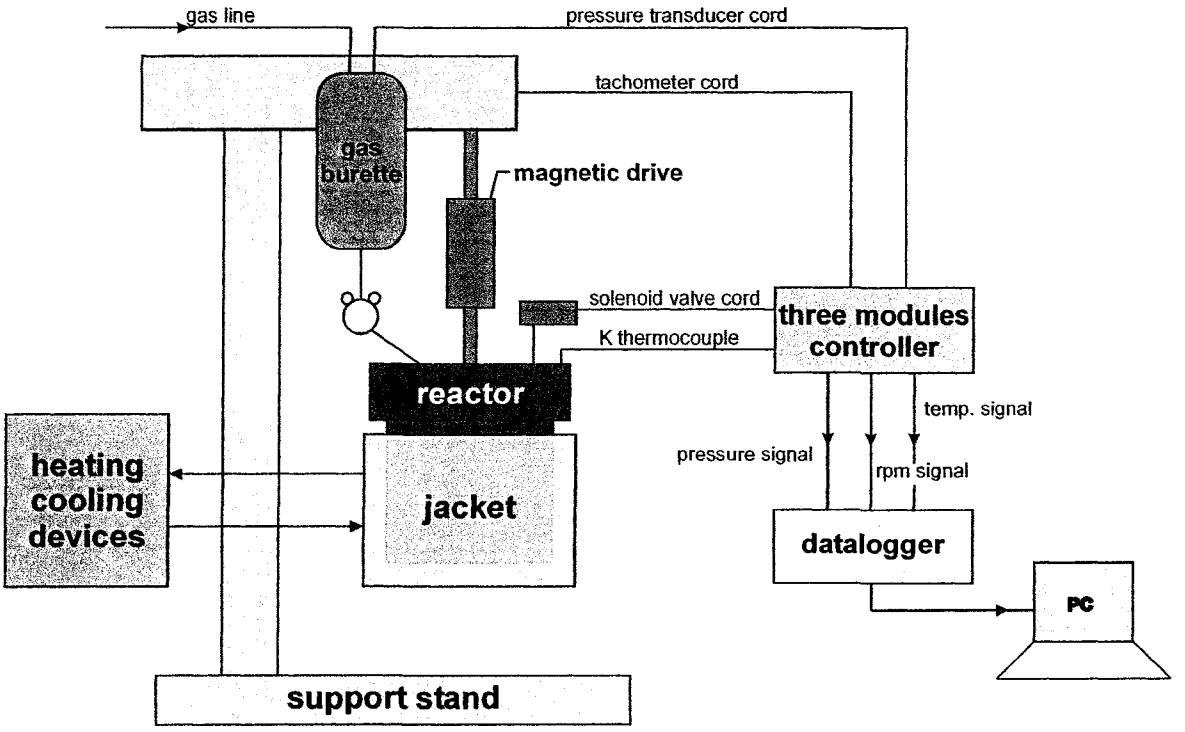

Figure 4.1 Schematic representation of polymerization reactor

Two reactor vessels are used depending on the pressure range (either a glass one for pressures up to 150 psi at 225 °C, or a stainless steel one for high working pressure up to 1000 psi at 225 °C). The glass vessel presents the advantage to allow direct visual observation of color or state changes. A detailed picture of the glass reactor is presented in Figure 4.2.

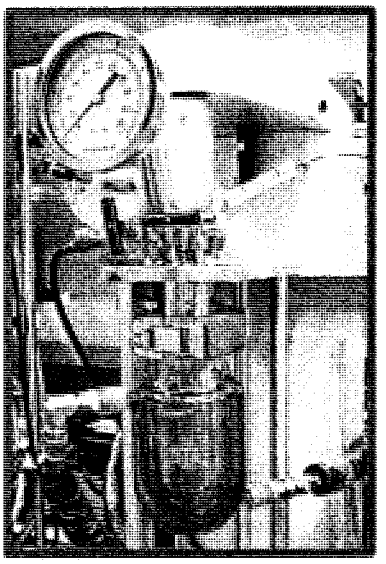

Figure 4.2 Glass reactor vessel to perform polymerization under a large range of temperature and pressure

As shown in Figure 4.2, the reactor head is equipped with a gas inlet and release valve equipped with a rupture disc for safety (rated for 150 psi, and to 1000 psi in the case of the steel vessel). The spring-loaded relief valve, which is adjustable between 50-150 psi, is a specific feature of the glass vessel, for added safety. The O-ring and the closure system ensure a tight glass-to-metal seal and support. The split ring for the glass vessel is padded with high temperature plastic cushions to prevent the glass vessel to come in direct contact with the metal split ring.[38]

The reaction vessel is jacketed in order to control the temperature. Heating and cooling is provided by an external PC-controlled circulator. In addition, an internal heating/cooling loop connected to a second external circulation bath is used for a better control of the polymerization temperature. A PC-controlled solenoid valve allows the fluid to flow through the loop when required, as monitored by an internal type-K

thermocouple. A detailed picture of the system for the set-up of internal temperature control is shown on Figure 4.3.

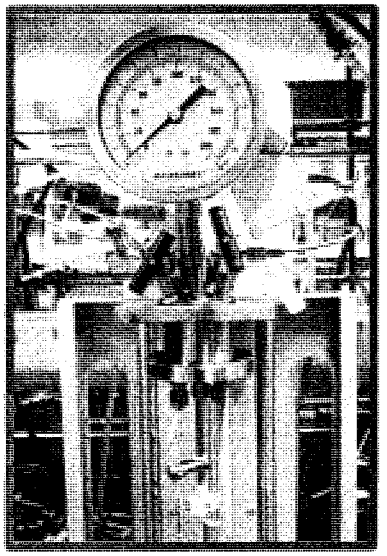

Figure 4.3 Reactor set-up for the internal temperature control

A one liter gas burette is used to measure the monomer consumption during polymerization by monitoring the burette pressure, as shown on Figure 4.4.

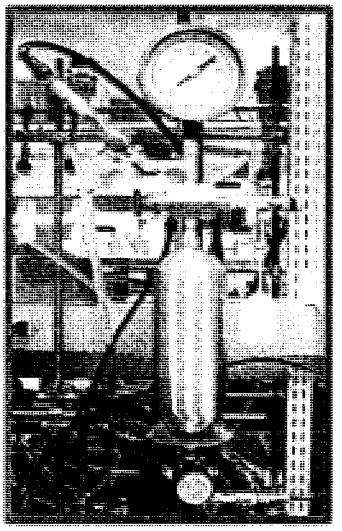

Figure 4.4 Gas burette for monomer consumption monitoring

Two internal stirrers are used: A standard turbine type stirrer or a gas entrainment impeller. The original turbine was modified to provide a good axial suspension of any solid particles to avoid mass transfer limitation. The gas entrainment impeller is the better choice for this purpose since it maximizes the diffusion of gaseous monomers into the solution. The gas is aspired through the hollow stirring shaft into the solution by centrifugal force at high stirring rates (Figure 4.5). The impeller is operated by an external motor linked through a magnetic coupling, eliminating any leak. The stirring speed can be adjusted through the Digital RPM Display Module.

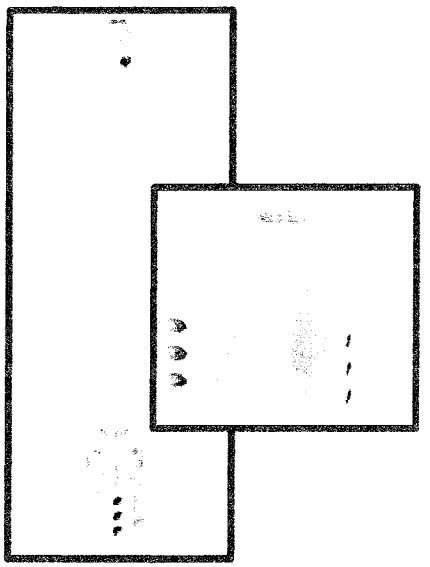

Figure 4.5 Gas entrainment impeller with the dispersion ports

This reactor set-up is completed by a three modules controller (Figure 4.6) which allows a full control and tuning of the reaction variables (pressure, temperature and stirring speed). A data logger (Figure 4.6) allows the recording of the real-time parameters on a PC.

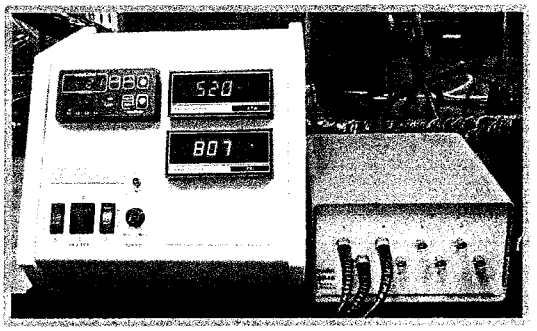

Figure 4.6 Three modules controller and data logger

A preliminary set of ethylene polymerization tests with the Cp_2ZrCl_2/MAO catalytic system was carried out to optimize experimental conditions. Unfortunately, the results of these preliminary tests showed poor reproducibility and inconsistent yields.[39]

After numerous improvements, detailed in the "Experimental" section (Chapter 3) both in the hardware (e.g., improvement of cooling system) and the experimental protocol (e.g., better cleaning and operating procedures), good reproducibility was finally obtained.

Several modifications, both in the hardware and in the experimental protocol, were performed in order to improve and stabilize the actual set-up. To avoid a potential deactivation of the catalytic system (which is well known for its sensitivity to impurities, even at the trace level), the reactor was pre-treated under vacuum and high temperature. Also, the system was purged before the monomer was fed to the system. To improve the experimental protocol and to ensure more consistent experimental conditions, separate pre-catalyst and co-catalyst stock solutions were prepared. Because MAO acts as an impurities scavenger[29], it was added to the reactor before the catalyst to trap impurities, thus allowing for the formation of a high number of active sites.

The amount of solubilized of ethylene must be known to correctly describe the kinetics of the polymerization reaction. Rempel *et al.* have measured ethylene solubility in toluene over a 293 – 343 K temperature range and over a 50 – 180 psi pressure range.[40] Because of the strong similarities between their method and ours, we used their results to determine the amount of dissolved ethylene in our calculations. The ethylene mass flow at various pressures was plotted against the reaction temperature, as shown on Figure 4.7.

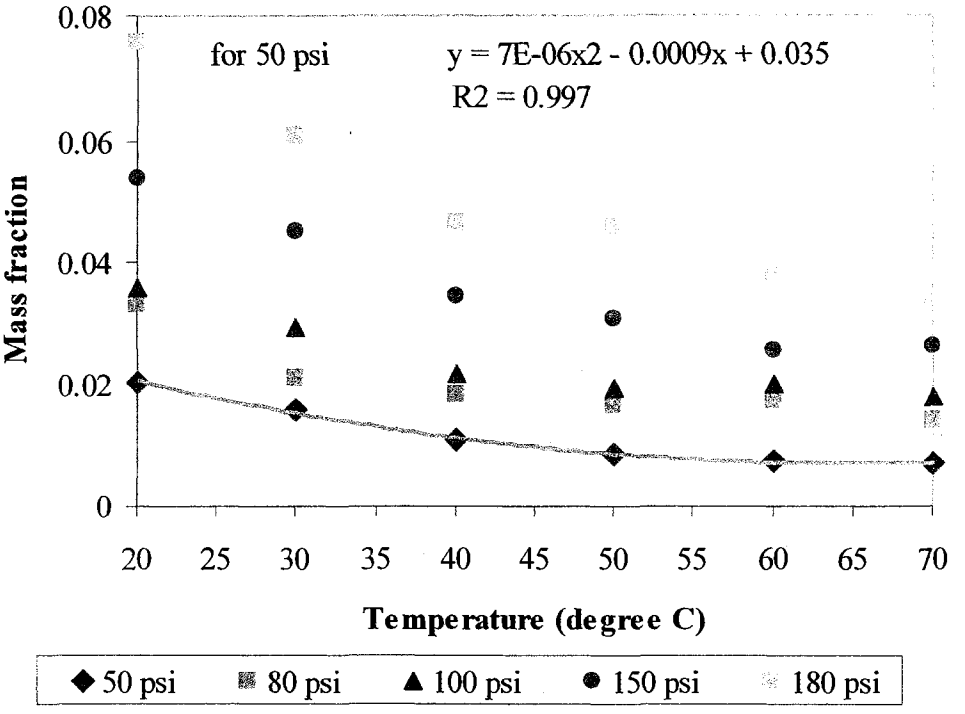

Figure 4.7 Ethylene mass fraction as a function of temperature

The Equation (1) for the plot at a pressure of 50 psi is:

$$y = 7E-06x^2 - 0.0009x + 0.035 \qquad \textbf{(1)}$$

The values of the actual conditions used in this work (T = 45 °C, p = 50 psi) were plotted in Equation (1), to obtain a mass fraction value, y, of 0.008675. The mass fraction value

was then transformed into mole fraction of ethylene by dividing the mass fraction by the molecular weight of the monomer ($M_{C_2H_4}$ = 28 g/mol) and the number of moles of ethylene (n = 0.0003) required for the solution saturation was then determined.

Further, for each run, the mole fraction calculated was subtracted from the total number of moles of ethylene calculated from the initial and final burette pressure values (moles of ethylene consumed during a reaction) using the ideal gas Equation (2),

$$\left(p_{in} - p_{fin}\right) * V = \Delta n * R * T \qquad (2)$$

where p_{in} is the initial monomer pressure, before the polymerization reaction (in psi), p_{fin} is the final monomer pressure, at the end of polymerization reaction (psi), V is the burette volume (L), Δn is the number of moles of monomer consumed during a reaction, R is the universal gas constant (8.3144 J mol^{-1} K^{-1}), and T is the room temperature (K). Once these modifications were completed, a new series of tests was undertaken, this time generating reproducible data. Figure 4.8 presents the pressure monomer profiles for four replicate ethylene polymerization tests performed with the modified set-up. The pressure profiles behave similarly and thus, we considered that a suitable stability and reproducibility was reached with our set-up.

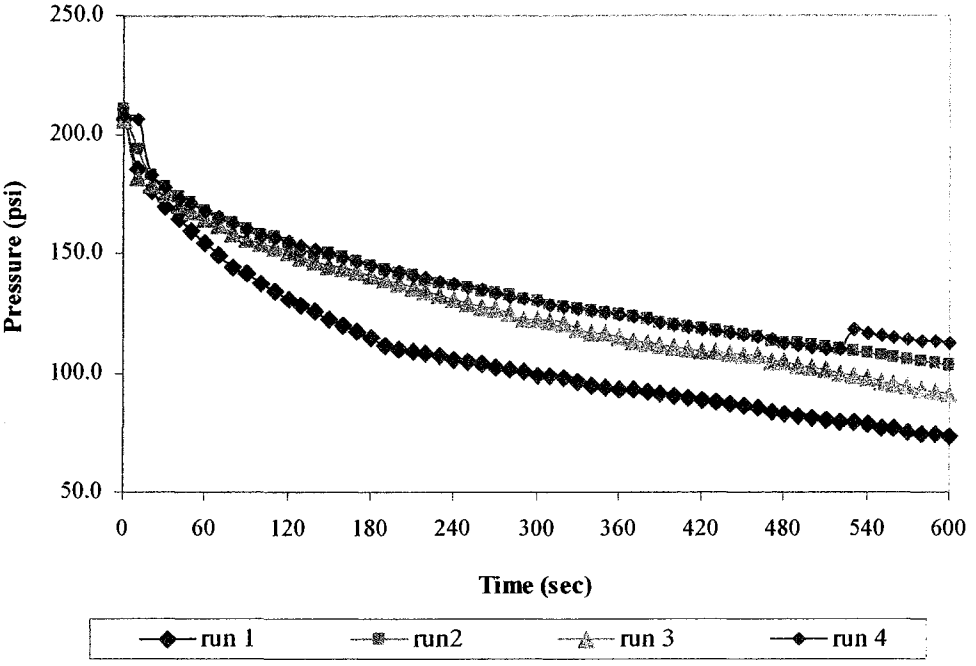

Figure 4.8 Reproducibility test for four replicate polymerization reactions at [Zr] = 5.5×10^{-5} mol L^{-1}, Al/Zr = 1000, T = 45 °C, monomer pressure = 2.2 bar, t = 10 min, toluene, 150 mL

Another approach that can be used to evaluate the process reproducibility is to calculate the reaction yields. In our study, reaction yields can be calculated using Equation (3):

$$yield\ (\%) = \frac{actual\ amount\ of\ polymer\ obtained}{theoretical\ amount\ of\ polymer\ to\ be\ obtained}\ x\ 100 \qquad (3)$$

Reaction yields for the tests that were carried out to verify the system stability and process reproducibility were thus calculated. As shown in Table 4.1, the obtained yield values also suggest good reproducibility of the process for the experimental conditions used ([Zr] = 5.5×10^{-5} mol L^{-1}, Al/Zr = 1000, T = 45 °C, monomer pressure = 2.2 bar, t = 10 min, toluene, 150 mL). The average yield for these runs is 87.96 ± 2.18%, for a relative standard deviation of only 2.48%.

Table 4.1 Ethylene homopolymerization yields in toluene

Run	(p_{in} - p_{fin}) (psi)	Mass C_2H_4 used (g)	Actual polymer mass (g)	Yield (%)
159	134.0	10.47	9.29	88.7
160	104.0	8.13	7.16	88.0
161	109.0	8.54	7.42	86.9
166	116.0	9.10	7.77	85.4
167	98.0	7.67	6.72	87.6
172	114.0	8.91	7.73	86.8
173	134.0	10.46	9.66	92.3

These tests were conclusive and allowed us to move further in the systematic study of the ethylene homopolymerization and the ethylene – α-olefin copolymerization in a hydrocarbon solvent (e.g., toluene).

Chapter 5 Homo- and co-polymerizatons in hydrocarbons

5.1 Homopolymerization in hydrocarbons

The polymerization of ethylene and ethylene – α-olefin copolymerization in toluene was studied using zirconocene dichloride (Cp_2ZrCl_2) and MAO as catalytic system. Even though some supplementary precautions must be taken when working with a gas under pressure manipulation at laboratory scale, ethylene was chosen as a model monomer because it is the simplest known olefin. Apart from being one of the most active catalytic system, the choice of a metallocene-based catalyst was also determined by the fact that the literature provides a lot of information related with its reaction mechanism and kinetics under various experimental conditions.[42]

As shown by our previous experience achieved during the tests performed to test system stability and process reproducibility, a standardized approach involving temperature control and catalyst activation must be used in order to conduct a systematic kinetic study and reduce to a minimum the potential sources of errors. In a typical polymerization experiment, the desired amount of freshly prepared stock solution of zirconocene dichloride in toluene, MAO solution in toluene and additional solvent are fed into the properly prepared reactor to fulfill the requirements of coordination polymerizations conditions for a given reaction temperature. After the system was purged with argon, the polymerization is started by the addition of the monomer at constant pressure. At the end of the polymerization time (t_f), the ethylene addition was stopped, the reactor depressurized and the reaction was quenched with an EtOH – HCl solution.

Any deviation from this general procedure, exact reaction conditions and all experimental data presented in charts are listed in Chapter 3.

Figure 5.1 shows a typical temperature and pressure variations profile for an ethylene polymerization test carried out under standardized conditions.

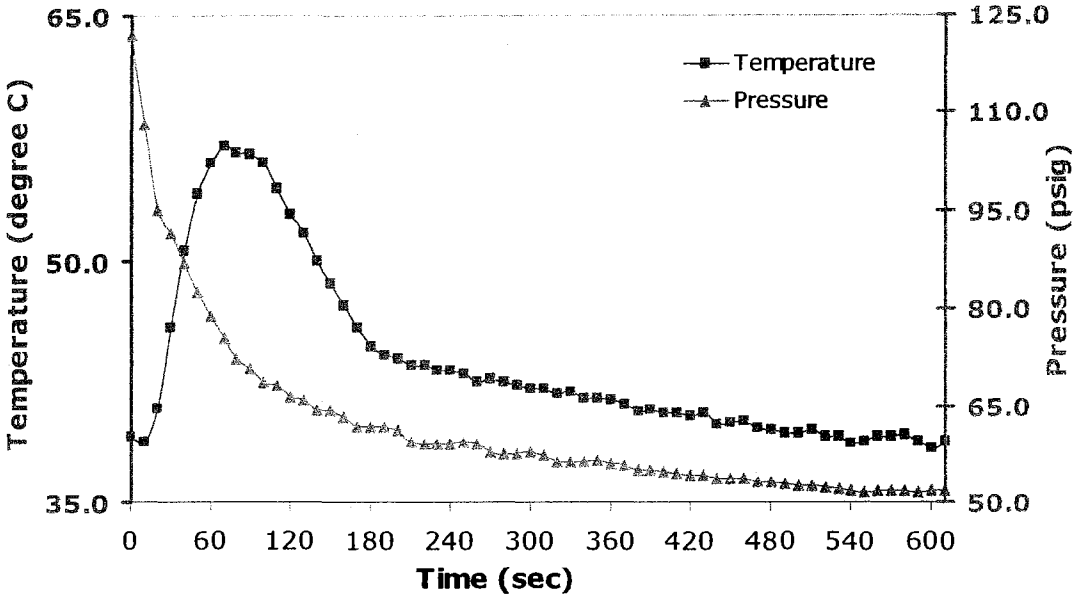

Figure 5.1 Temperature and pressure profiles during a typical ethylene polymerization reaction

The monomer pressure profile evolves from a decay-type curve to a steady-state type one during the reaction. In comparison, after a very short induction period, the temperature increases and then decreases rapidly. The maximum temperature corresponds to the steeper region of the pressure curve in connection with the increased monomer consumption. This evolution can be explained if two processes are considered to take place simultaneously: Monomer saturation of the solvent and polymerization. The same

behavior has also been noticed in other kinetics studies.[37] In working conditions similar to those used in our experiments, Hamielec *et al.* noticed that the rate of monomer consumption near time zero rapidly increased, followed by a slow decrease in reaction rate. Also, an induction period was detected.[37]

The polymerization system is homogenous only at the very beginning of the process. To express the transfer to the heterogeneous phase, in a diffusion-controlled process, Janiak *et al.*[41] proposed an equation in which the active species formed in homogeneous conditions exist in a complexation equilibrium with the active complex embedded in a polymer matrix. This equilibrium favors the formation of active species under homogeneous conditions only for large [Al]/[Zr] ratios. However, the increased amount of precipitated polymer results in a steady decline of the polymerization rate.

In a study on propylene polymerization using Cp_2ZrCl_2/MAO, Rempel *et al.*[42] also noticed a severe decay in the polymerization rate, followed by steady state conditions. Based on this observation, they concluded that the active species were in dynamic equilibria with some type of dormant species. The amount of MAO used in the experiment plays a critical role not only in the initial catalyst activity, but also on the rate of catalyst deactivation, the duration of steady state and the late behavior in catalyst activity. MAO plays a positive role by activating the catalyst and keeping the active species alive. Meanwhile, MAO is involved in deactivation reactions as dimerization of active zirconocene complexes and its complexation to the active sites.

Other studies on ethylene polymerization suggest that the shell of polymer formed around catalyst particles prevents the free access of monomers to the active sites and imposes a limitation on monomer diffusion.[1] Such polymerization taking place layer by

layer results in an onion-type internal polyethylene morphology. This mechanism of particle growth is associated with a kinetic profile in which an initial induction period is followed by an acceleration period, after which, in the absence of chemical deactivation, a stationary rate is obtained.

The assessment of catalyst activities represents a starting point when comparing system with varying experimental conditions (e.g., polymerization duration, process temperature, type of solvent, etc.). Along with turnover number (TON) and turnover frequency (TOF), catalyst activity is widely used to estimate catalyst efficiency. Catalyst activity, TON and TOF can be calculated using the equations (4), (5) and (6), respectively.

$$activity = \frac{kg\ of\ polymer\ produced}{(mol\ of\ catalyst)\ hour\ bar} \qquad \textbf{(4)}$$

$$turn\ over\ number\ (TON) = \frac{mol\ monomer}{mol\ catalyst} \qquad \textbf{(5)}$$

$$turn\ over\ frequency\ (TOF) = \frac{mol\ monomer}{(mol\ catalyst)\ hour} \qquad \textbf{(6)}$$

Using equations (1), (2) and (3) and the experimental conditions: [Zr] = 5.5×10^{-5} mol L^{-1}, Al/Zr = 1000, T = 45 °C, monomer pressure = 2.2 bar, t = 10 min, toluene, 150 mL, stirring = 1200 rpm, activity, TON and TOF were calculated and compared. As shown in Table 5.1 the values obtained for several runs under the above conditions show consistent values, and again suggest a good reproducibility of the process.

Table 5.1 Activity, TON and TOF for ethylene homopolymerization in toluene

Run	Activity kg(PE)[mol(catZr)hbar]$^{-1}$	TON ($molC_2H_4/molZr$)	TOF ($molC_2H_4$ $molZr^{-1}$ h^{-1})
159	3071	45359	272153
160	2367	35251	211508
161	2453	36996	221976
166	2569	39425	236551
167	2221	33251	199508
172	2555	38589	231534
173	3193	45328	271970

5.2 Effect of reaction time on ethylene polymerization

The influence of the polymerization time over the polymerization yield was also investigated. The polymer yield was calculated using equation (3) in Chapter 4, and the values obtained are presented in Table 5.2.

Table 5.2 Effect of polymerization time over the polymerization yield

Run	Polymerization time (min)	(p_{in} - p_{fin}) (psi)	Mass of C_2H_4 used (g)	Actual polymer mass (g)	Yield (%)
175	40	194.0	15.18	12.07	79.5
162	30	168.0	13.15	10.34	78.6
174	20	132.0	10.35	8.65	83.6
176	1	43.0	3.35	3.87	(~100.0)

When the polymerization time is increased from very short (e.g., 1 minute) to longer ones (e.g., 40 minutes), the polymer yield is decreasing. Such results can be explained if we consider that during the initial stages of polymerization the process is homogeneous, which facilitates free monomer access to the catalytically active centers. When the polymer starts to form and embeds the active species, the process becomes diffusion controlled.

Using the equations (4), (5) and (6), respectively, the activity Cp_2ZrCl_2/MAO catalytic system was calculated for our working conditions when polymerization duration was varied between 1 and 40 minutes. The values obtained in this series of experiments are presented in Table 5.3.

Table 5.3 Effect of polymerization time over catalyst efficiency parameters

Run	Polymerization time (min)	Activity kg(PE)[mol(catZr)hbar]$^{-1}$	TON ($molC_2H_4/molZr$)	TOF ($molC_2H_4$ $molZr^{-1}*h^{-1}$)
175	40	998	65735	98603
162	30	1139	56964	113927
174	20	1430	44848	134544
176	1	12793	14555	873328

For the catalyst activity, a similar trend as in polymer yield study was observed (Figure 5.2): higher values are obtained for shorter polymerization times. However, when the process is diffusion controlled, the catalyst activity is decreasing.

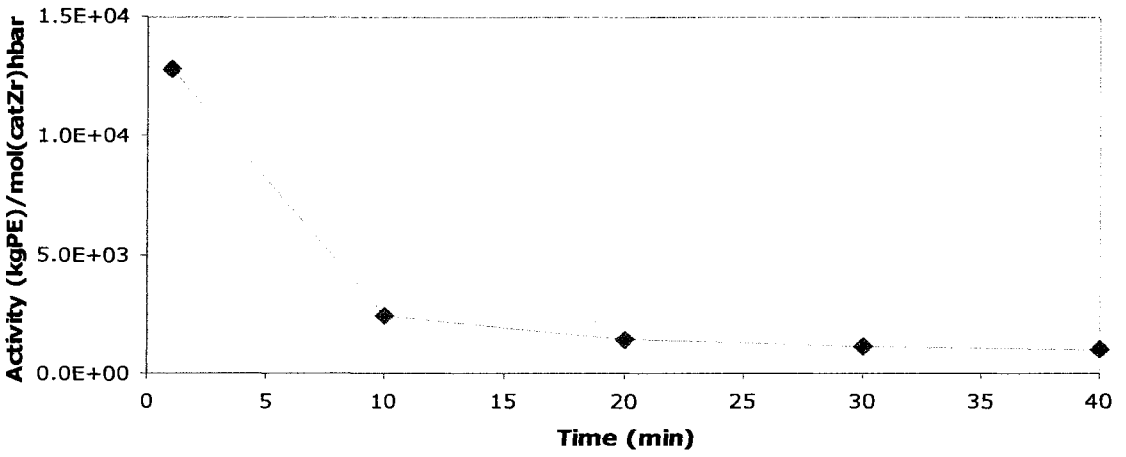

Figure 5.2 Catalyst activity plot for different polymerization times

The calculated values for TOF and TON also show a good correlation. As it can be seen on Figure 5.3, when polymerization time increases, TOF is inversely proportional to TON. This trend can be explained by the fact that TOF is obtained by dividing the amount of monomer consumed at longer polymerization times, when the number of moles of catalyst does not vary.

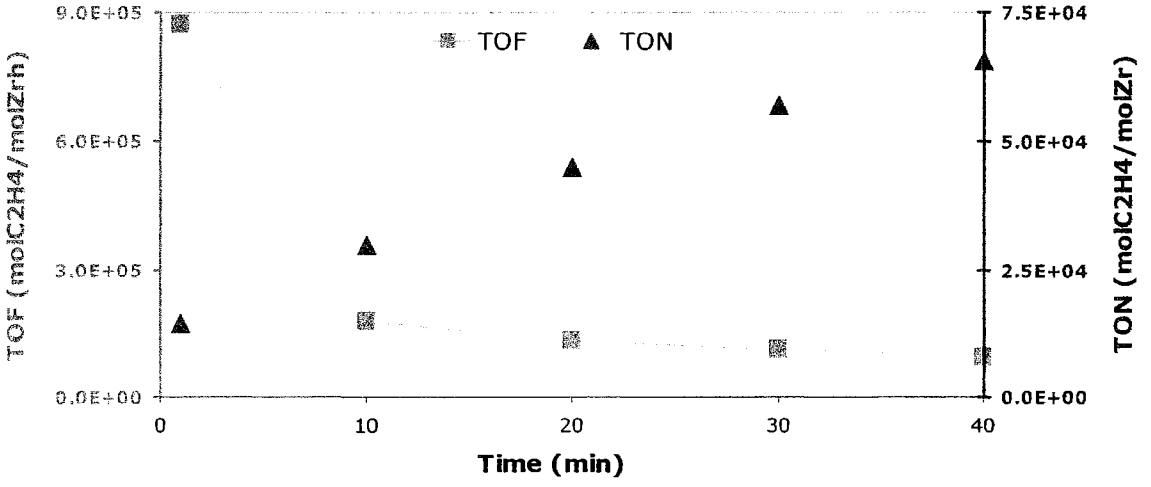

Figure 5.3 TON and TOF values plotted for different polymerization times

We were also interested in investigating any potential effect of polymerization duration on polyethylene properties. Differential Scanning Calorimetry (DSC) was the method used to determine the melting temperature (T_m) and polymers crystallinity (%). These results are presented in Table 5.4 and show that melting temperature and crystallinity are not affected by the duration of the process. This observation suggests that the first minutes of the process, when the reaction still evolves under homogeneous conditions and monomer molecules still can easily access the active species, are determinant for polymer properties such as melting temperature and crystallinity.

Table 5.4 Effect of polymerization time on T_m and crystallinity

Polymerization time (min)	**T_m (°C)**	**Crystallinity (%)**
1	138.1	41.8
10	138.6	43.2
20	140.1	36.4
30	141.1	40.8
40	139.3	42.3

Due to their high degree of crystanillity, the polyethylenes synthesized in our working conditions were expected to be brittle. Their semi-crystalline structure suggests that high temperatures, higher than their melting temperature, are required for their processing.

5.3 Effect of temperature on ethylene polymerization

The effect of temperature on ethylene polymerization was also studied. The results for the polymer yield at various temperatures are presented in Table 5.5.

Table 5.5 Effect of temperature on the polymerization yields

Run	Polymerization temperature (°C)	(p_{in} - p_{fin}) (psi)	Mass C_2H_4 used (g)	Actual polymer mass (g)	Yield (%)
210		66.0	5.18	5.68	(~100.0)
212	70	80.0	6.25	5.30	84.8
213		69.0	5.38	3.93	73.0
207		93.0	7.28	6.90	94.8
208	60	79.0	6.17	5.45	88.4
209		91.0	7.10	7.04	99.2
159		134.0	10.47	9.29	88.7
160	45	104.0	8.13	7.16	88.0
161		109.0	8.54	7.42	86.9
214		91.0	7.04	5.91	84.0
215	30	114.0	8.87	8.90	(~100.0)
216		112.0	8.71	8.98	(~100.0)
217	20	97.0	7.53	7.54	(~100.0)

To better evaluate the influence of temperature over catalyst efficiency, the activity, TON and TOF of Cp_2ZrCl_2/MAO catalytic system were also calculated for the same polymerization temperatures. These results are presented in Table 5.6.

Table 5.6 Effect of polymerization temperature on catalyst efficiency

Run	Polymerization temperature (^{0}C)	Activity kg(PE)[mol(catZr)hbar]$^{-1}$	TON ($molC_2H_4/molZr$)	TOF ($molC_2H_4$ $molZr^{-1}*h^{-1}$)
210		1878	22439	134635
212	70	1752	27098	162589
213		1299	23317	139903
207		2281	31523	189137
208	60	1802	26723	160341
209		2327	30752	184510
159		3071	45359	272153
160	45	2367	35251	211508
161		2453	36996	221976
214		1934	30536	181403
215	30	2942	38459	230757
216		2969	37747	226481
217	20	2493	32713	196280

Finally, TON and TOF trends are presented for different process temperatures in Figure 5.4.

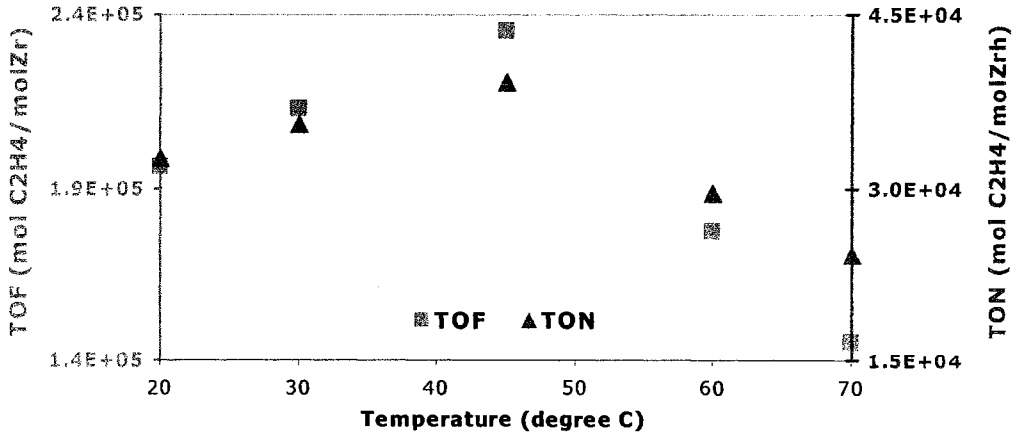

Figure 5.4 TON and TOF values for different polymerization temperatures

As can be noticed from Figure 5.4, TOF and TON reached a peak at temperatures between 40 and 50 °C and decreased outside of this range. This thermosensitivity of the Cp_2ZrCl_2/MAO catalytic system at temperatures higher than 50 °C is a common feature of most metallocene based catalysts. Different deactivation reactions can be responsible for metallocene catalysts instability, but it seems that impurities play a determinant role at higher temperatures. Due to hydrogen transfer reactions between alkylated zirconocene or MAO, inactive complexes as Zr-CH_2-Zr or -Al complexes are formed. The excess of MAO and alkyl exchange can reactivate the inactive complexes, but the transformation is irreversible if the cyclopentadienyl ring is split off, a reaction that is more likely to take place in the case of unbridged metallocene than in ansa-metallocene.[43]

The effect of temperature on the properties of polymers synthesized at different temperatures was also studied. The values obtained for the melting temperature (T_m), polymers crystallinity (%) and transition glass temperature (T_g) are presented in Table 5.7.

Table 5.7 Effect of temperature on T_m , crystallinity and T_g

Polymerization temperature (°C)	**T_m (°C)**	**Crystallinity (%)**	**T_g (°C)**
70	138.0	26.3	-
60	140.5	24.9	87.4
45	138.6	32.6	84.0
30	138.8	7.5	81.6
20	141.8	3.7	87.6

Properties like T_m and T_g are not significantly affected by variations of the reaction temperatures as similar values were obtained when the temperature was varied between 20 and 70 °C. For the crystallinity, a variation can be noticed with a peak at 32.6% for a working temperature of 45 °C. At working temperatures of 30 and 20 °C the degree of crystallinity decreased to 7.5% and 3.7%, respectively. Such low values for crystallinity suggest an amorphous polymer structure.

Polymers crystallization can be understood from the thermodynamics of the process. When the polymer is melted, the polymeric chains are entangled in a random coil configuration, a state which is entropy-controlled. Cooling the melted polymer at lower rates allows the molecules to arrange themselves in a regular way and a state of minimum free energy is reached. If the cooling rate is very fast then the polymer may not crystallize and a completely amorphous polymer can be obtained. The process in this case is kinetically controlled.

5.4 Activation energy calculation

The investigation of the kinetics of ethylene polymerization at different temperatures was further pursued through an attempt to calculate the activation energy of the process in our working conditions. The Arrhenius equation (Equation 7), which correlates the rate constant of the process (k) with temperature (T) at which the reaction takes place, represents the starting point of our calculation:

$$k = A\, e^{-E_a / RT} \qquad (7)$$

where k is the rate constant of the reaction, A is a pre-exponential factor, E_a is the activation energy of the process, R is the universal constant gas (8.3144 J mol^{-1} K^{-1}), and T is the absolute temperature (K). Taking the natural logarithm of the Arrhenius equation yields Equation (8):

$$\ln k = \ln A - \left(\frac{E_a}{R}\right)\frac{1}{T} \qquad \textbf{(8)}$$

However, the rate constant, k, can be substituted by the catalyst activity, which is also in a rapport of direct proportionality with the reaction rate, r_p, (Equation 9).

$$\textit{Catalyst activity} \sim r_p \sim k \qquad \textbf{(9)}$$

Taking into account Equation 9, the rate constant, k, can be replaced in Equation (8) by catalyst activity. Then the logarithm of the catalyst activity (ln activity) determined for different temperatures was plotted in function of 1/T, ln activity = f (1/T), as shown on Figure 5.5.

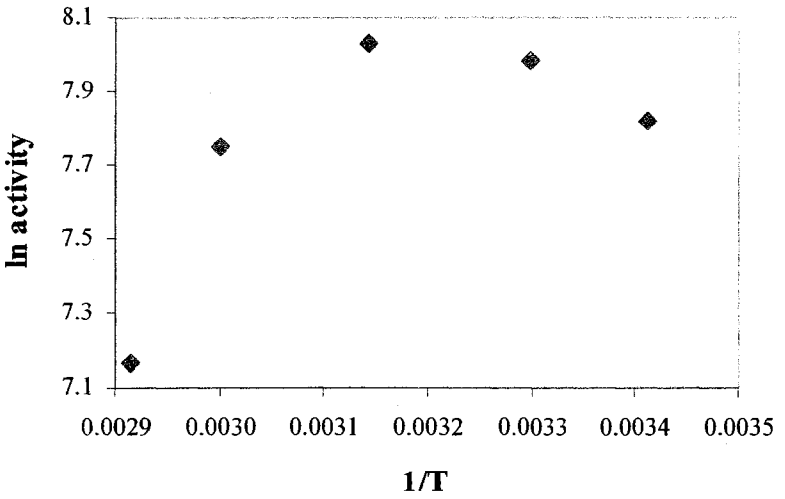

Figure 5.5 Arrhenius plot for ethylene polymerization

For calculation purposes, only the values obtained for temperatures between 20 and 45 °C were considered in the following steps (below). The relationship (Equation 8) between (ln activity) and 1/T was determined using the linear regression of the Arrhenius plot, as shown on Figure 5.6.

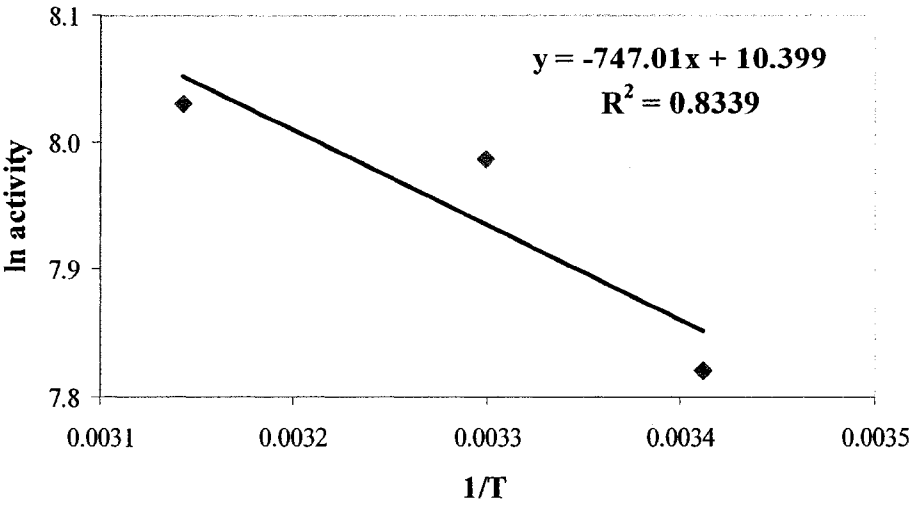

Figure 5.6 Arrhenius plot for temperatures between 20 and 45 °C

Considering the Equations 8 and 10:

$$y = -747.01\,x + 10.399 \qquad \textbf{(10)}$$

and the general Equation 11:

$$y = -m\,x + b \qquad \textbf{(11)}$$

y can be assimilated with *(ln activity)* and the slope, m, with (E_a/R). From here, a value of 6.2 KJ/mol was calculated for the activation energy (E_a).This value has to be interpreted with caution because of the uncertainty associated with the calculations (most notably,

the low number of points, *n*). Under different working conditions (e.g., higher [Al]/[Zr] ratio), a recently published literature value is equal to 14 Kcal/mol, or 58.5 KJ/mol.[44]

5.5 Copolymerization in hydrocarbons

As part of the copolymerization part of this study, ethylene – α-olefin copolymerization in toluene was investigated in the presence of zirconocene dichloride (Cp_2ZrCl_2) and MAO as the catalytic system, while 1-hexene was chosen as the comonomer. The much easier manipulation at the laboratory scale and the possibility to obtain a defined concentration in homogeneous solutions were the advantages brought by the liquid state of 1-hexene. Due to a much slower polymerization rate compared to that of ethylene, diffusion limitations in 1-hexene polymerization less likely.

The same standard methodology (temperature control and catalyst activation) as in the homopolymerization experiments was used in order to conduct a systematic kinetic study and reduce at minimum the potential sources of errors. Again, the comonomer was injected in the system before the ethylene monomer, and 1-hexene concentrations of 0.2, 0.5 and 0.8 mol L^{-1} were used. Copolymerization reproducibility for any concentration of comonomer concentration was assessed in the same way as for ethylene polymerization.

Figure 5.7 presents a typical profile for the variations in temperature and pressure during an ethylene – 1-hexene copolymerization run.

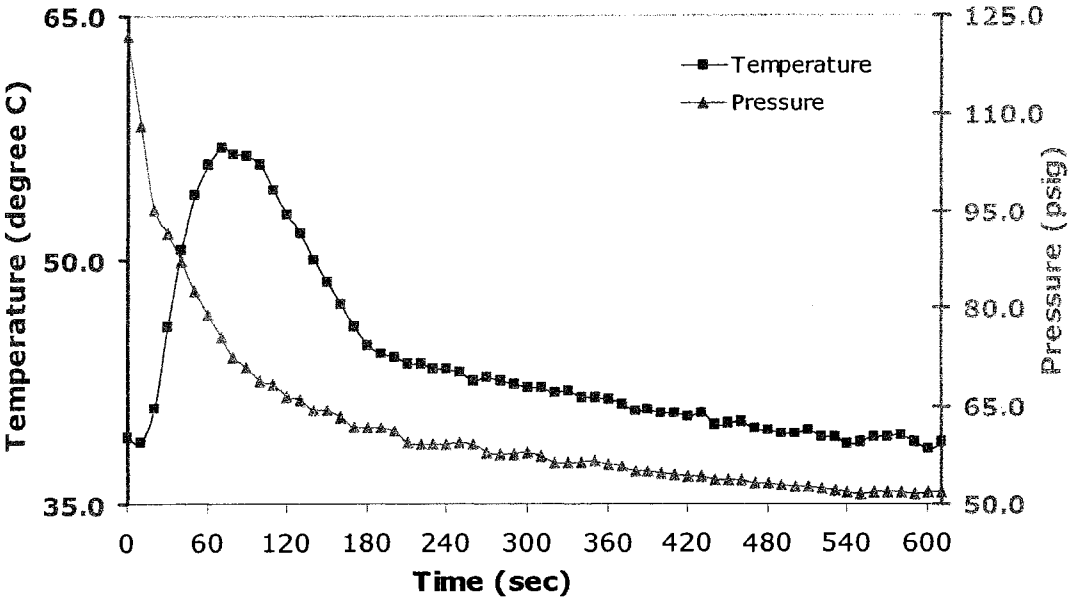

Figure 5.7 Temperature and pressure profiles during a typical ethylene – 1-hexene copolymerization test

As shown on Figure 5.7, the temperature and pressure profiles during a typical ethylene – 1-hexene copolymerization run are similar to those obtained during the ethylene polymerization runs. Again, monomer pressure profile evolves from a decay-type curve to a steady-state type one. Differences can be noticed at the exothermal level for the temperature plot and a much smoother evolution of monomer pressure profile.

These differences can be explained by the presence of two monomers in the reaction medium and their competition for the available catalytic active species. The ethylene pressure profile is in agreement with other data reported in the literature: using Cp_2ZrCl_2/MAO as the catalytic system, Chien *et al.*[45] conclude that the R_p of the ethylene/hexane copolymerization reaction is always smaller than the R_p for the ethylene

polymerization reaction. Therefore, there seems to be a negative "comonomer effect", which means that the presence of the α-olefin does not enhance the ethylene polymerization rate. A slower migratory insertion rate of hexane into transition metal-polymer chain compared to that of ethylene is responsible for this evolution. The rate enhancement upon 1-hexene addition, reported by Koivumäki and Seppälä, was seen only when the newly synthesized polymer was insoluble in the reaction medium. In this case, no growing and agglomerating polymer particles and no mass transfer limitations were present.[46]

A first step of the kinetics study in a case of ethylene – 1-hexene copolymerization was to evaluate the influence of polymerization duration on polymer yield and catalyst efficiency. To calculate the polymer yield the reaction yield equation (Equation 3 from Chapter 4, *Reactor design, set-up and system stability*) was used. The results of these tests are presented in Table 5.8.

Table 5.8 Ethylene – 1-hexene copolymerization yields

Run	$[C_6H_{12}]$ mol L^{-1}	Polymerization time (min)	Mass C_2H_4 used (g)	Mass C_6H_{12} used (g)	Theoretical polymer mass (g)	Actual polymer mass (g)	Yield (%)
132	0.2	10	7.04	2.80	9.84	8.40	85.3
131		30	4.93		7.73	5.40	69.8
119	0.50	10	5.55	6.30	11.85	5.12	43.2
129			3.43		9.73	2.74	28.1
130		30	3.68		9.98	2.94	29.5
121	0.8	10	2.73	10.08	12.81	1.86	14.5
122			3.05		13.13	3.05	23.2
123			3.52		13.62	3.16	23.2
128		30	2.97		13.05	2.50	19.2
126			4.46		14.54	3.22	22.1

As suggested by the data from Table 5.8, higher polymer yields are obtained when lower comonomer concentrations (e.g., 0.2 mol L^{-1}) and shorter polymerization times are used. In our working conditions, a negative comonomer effect is thus noticed.

Catalyst efficiency was also investigated. Activity, TON and TOF were calculated using same equations as for the ethylene polymerization reaction. The results are presented in Table 5.9.

Table 5.9 Catalyst efficiency parameters in ethylene – 1-hexene copolymerization

Run	$[C_6H_{12}]$ mol L^{-1}	Polymerization time (min)	Activity kg(PE)[mol(catZr)hbar]$^{-1}$	TON ($molC_2H_4/molZr$)	TOF ($molC_2H_4$ $molZr^{-1}*h^{-1}$)
132	0.2	10	287	30527	3053
131		30	61	20987	700
119	0.5	10	175	24058	2406
129			93	14904	1490
130		30	33	15947	532
122	0.8	10	104	13224	1322
123			106	15258	1502
128			85	12893	1289
126		30	37	19353	645

The catalyst efficiency parameters are affected by the presence of two monomers in the reaction medium and by their competition for the available catalytic active species. Activity, TON and TOF all decrease with increasing comonomer concentration, a relationship that becomes more evident at longer polymerization times.

Copolymers properties were also evaluated using the DSC technique. The values obtained for T_m and crystallinity are presented in Table 5.10.

Table 5.10 Effect of polymerization time on copolymers T_m and crystallinity

$[C_6H_{12}]$ mol L^{-1}	T_m (°C)		Crystallinity (%)	
	10 min	30 min	10 min	30 min
0	139.1	139.5	45.5	30.5
0.2	121.9	122.8	20.8	24.9
0.5	113.6	116.0	22.6	24.2
0.8	107.0	108.7	17.1	22.0

As expected, the presence of another comonomer in the system affects copolymer properties such as T_m and crystallinity, an influence which is more noticeable for longer polymerization times. When concentration of 1-hexene is increased from 0 to 0.8 mol L^{-1}, bothT_m and crystallinity decrease. This evolution is due to the incorporation of small amounts of comonomer into the polyethylene main chain and results in lower crystallinity and melting temperature, as well as higher flexibility processability and toughness, which are all characteristics intensely exploited by the polymer industry.

Another interesting aspect of the project was to evaluate the amount of comonomer incorporated in the main polymeric chain, which was done by analyzing the copolymers compositions using a FT-IR technique described in the literature: calibration curves were prepared using polyethylene-polyhexene blends (for copolymers with a low hexane content), and with ^{13}C-NMR for the copolymers with a high hexane content.[34] The amount of comonomer incorporated in the copolymers was determined using the calibration curves and A_{1380}/A_{722} absorbance ratios. Asymmetrical and symmetrical bending vibrations of C-H bonds in methyl groups ($-CH_3$) groups produce infrared bands near 1450 cm^{-1} and 1375 cm^{-1}; however, when two or three methyl groups are present on the same carbon, the symmetrical bending band is split into two or more closely spaced

peaks near 1385 cm^{-1} and 1370 cm^{-1}. The band near 720 cm^{-1} is characteristic for methylene groups ($-CH_2-$); its intensity increases in proportion to the number of adjacent methylene groups. It thus indicates the presence of unbranched long-chain alkanes.

These results are presented in Table 5.11.

Table 5.11 Comonomer content in ethylene – 1-hexene copolymers in toluene

Run	$[C_6H_{12}]$ mol L^{-1}	A_{1380}/A_{722}	Hexene content, c_{hexene} (%)
132	0.2	0.38	8.1
131		0.07	1.7
119	0.5	0.49	9.9
129		0.29	6.8
130		0.35	7.5
121	0.8	0.44	9.3
122		0.31	6.9
123		1.01	-
128		0.57	9.5
126		1.18	-

This attempt was judged not very successful because the results obtained were not consistent. Considering the values measured for copolymers melting temperature and crystallinity, we would expect that the amount of incorporated comonomer to increase when higher amounts of 1-hexene would be present in the system. The inconsistency of the results obtained using the FT-IR technique can be explained by an inconsistent sample preparation (e.g., sample film thickness). Other methods that can be used to determine the amount of comonomer incorporated are ^{13}C-NMR (e.g., for higher comonomer content) and gel permeation chromatography.

Chapter 6 Homo- and co-polymerizatons in fluorous biphasic system

6.1 Homopolymerization in fluorous biphasic system

Even though fluorocarbons (FC) and hydrocarbons (HC) are chemically similar, they present totally different structures and properties. Fluorine is the most electronegative element in the periodic table, and it has a large van de Waals radius (1.47 Å *vs* 1.20 Å for H), a high ionization potential and a very low polarizability.[47] These properties reduce the conformational freedom of fluorinated tails that are bulky and rigid, arranged in a typical helical conformation (depending on temperature), with a dense electron-rich coating that prevents chemical and biochemical attacks.[48] Due to these characteristics, FC possesses strong intramolecular (covalent) bonding and very weak intermolecular (van der Waals) interactions, properties which make FC more stable than their corresponding HCs, with low surface tensions, high fluidities and densities, low dielectric constants and refractive index, high vapor pressures, high compressibilities and high gas solubilities. [47] Being chemically and biochemically inert, FC are used in different fields, such as in biomedical applications. For example, they can be used as oxygen carrier in blood substitutes, in the aerobic conservation of transplant organs, in cancer therapy, in ophthalmology, in diagnostic procedures and in bone reconstruction.[49]

Fluorine chemistry has also found applications in clean chemical synthesis, or *green chemistry*, a field in which highly efficient chemical reactions are developed in order to produce little or no waste. In fact, this approach ensures that as much of the substrates and reagents as possible find their way into the final products, and that the use

of auxiliary compounds such as solvents and promoters is minimized or eliminated.[50] However, cholorofluorocarbons (CFCs) have been involved in some of the more negative aspects of the chemical industry; they were identified as playing a significant role in the ozone layer depletion and they were phased out as a result of the 1987 Montreal Protocol.[50]

Perfluorocarbons (PFC) are a class of perfluororinated and aliphatic compounds such as perfluoroalkanes, perfluoroalkyl ethers and perfluoroalkylamines, which, besides the fact they are suitable for heat transfer and for temperature control, can be used as a immiscible reaction medium in the presence of hydrocarbon and more polar organic solvents.[15] This particular property has led to the development of fluorous biphasic chemistry (FBS) and other fluorous solvent technology. The principle behind FBS technology is based on the immiscibility of compounds containing perfluoroalkyl groups with hydrocarbons at low temperatures, but which upon heating become a single phase allowing the reaction to proceed under homogeneous conditions. Lower temperatures cause phase separation and allow solvent and catalyst separation from the product. This temperature dependent behavior of FBS technology improves product or catalyst separation, gives better efficiency and reduces wastes. [47, 51]

Inspired by the properties of the FBS technology, we conducted a system kinetic study of ethylene polymerization in the presence of a mixture of FC 72 (primarily compounds with six carbons, e.g., perfluoro-n-hexane) and toluene (FC 72: toluene = 1:4, v/v). Zirconocene dichloride (Cp_2ZrCl_2) and MAO were used as the catalytic system. Polymerization experiments under FBS conditions were undertaken in order to probe a possible effect of fluorous biphasic conditions on process kinetics and

catalyst activity. Also, this investigation allows optimizing the polymerization activities of the catalytic system through the comparison with the experimental results in a pure hydrocarbon solvent (e.g., toluene). The same standard methodology involving temperature control and catalyst activation used during polymerization experiments in toluene was also applied under FBS conditions. The perfluorinated solvent was injected before the ethylene was admitted in the system.

Figure 6.1 shows a typical profile for the variations in temperatures and pressures during an ethylene polymerization test in FBS conditions.

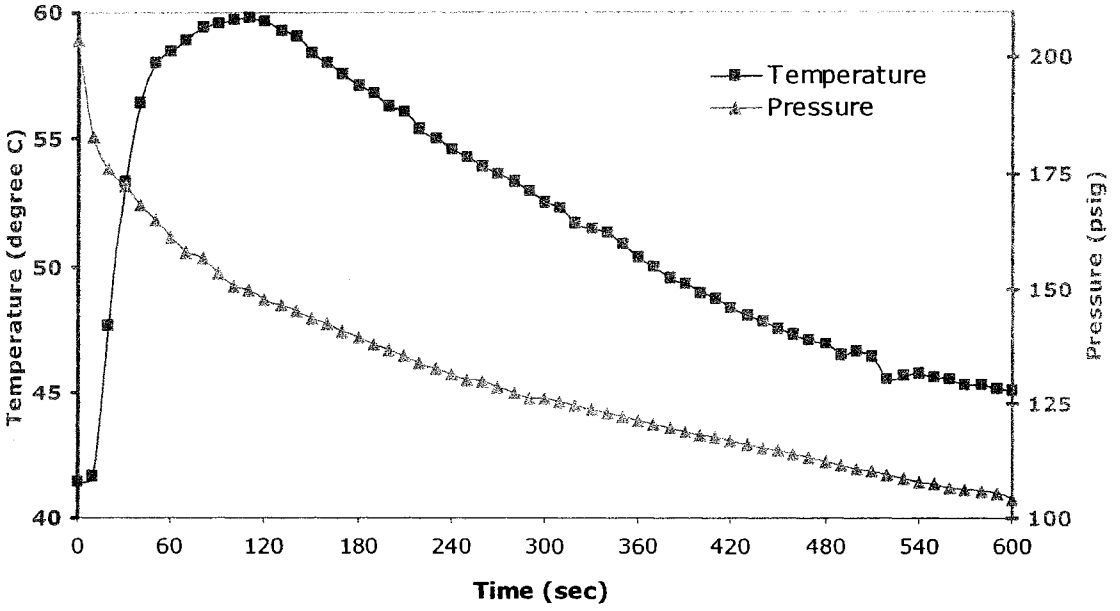

Figure 6.1 Temperature and pressure profiles during a typical ethylene polymerization in FBS conditions

During ethylene polymerization under FBS conditions, the monomer pressure profile evolves again from a decay-type curve to a steady-state type one. After a very

short induction period, the temperature profile follows the same trend as the one obtained when toluene was used as reaction medium: an increasing trend followed by a decreasing one. Again, the maximum temperature reached corresponds to a steeper region on the pressure curve in connection with the increase in monomer consumption.

Under FBS conditions, the polymerization process is truly homogeneous only at the very beginning, when the polymer is precipitating very rapidly under the working conditions used in this set-up. Because the active species are trapped in the insoluble polymer matrix, the process is diffusion controlled. Due the particular properties of the FBS system, PFC present in the system acts as an inert diluent which keeps the active complex out of the growing polymer matrix, thus minimizing monomer diffusion limitations.

Equation 3, Chapter 3 was used to calculate the polymer yields obtained in FBS conditions. The results are presented in Table 6.1.

Table 6.1 Ethylene polymerization yields in FBS conditions

Run	(p_{in} - p_{fin}) (psi)	Mass C_2H_4 used (g)	Actual polymer mass (g)	Yield (%)
178	93.0	7.28	7.22	99.2
179	99.0	7.73	7.72	99.9
198	106.6	8.34	8.32	99.8
202	107.1	8.36	8.30	99.2
203	87.0	6.78	6.76	99.7

Even when FBS conditions were introduced, good polymer yields were obtained. The yield values are consistent and indicate that the coordination polymerization of the process is high reproducible even when the reaction conditions are changed. We can also

conclude that FBS conditions are compatible with coordination polymerization conditions and that FC 72 is inert with respect to MAO.

Another interesting component of our kinetic study was the evaluation of the influence of FBS conditions on the catalyst efficiency. Using the Equations 4, 5 and 6 in Chapter 5, activity, TON and TOF were calculated and are presented in Table 6.2.

Table 6.2 Catalyst efficiency parameters in FBS conditions

Run	Activity kg(PE)[mol(catZr)hbar]$^{-1}$	TON ($molC_2H_4/molZr$)	TOF ($molC_2H_4$ $molZr^{-1}*h^{-1}$)
178	2387	31534	189201
179	2552	33489	200933
198	2750	36145	216869
202	2744	36241	217446
203	2235	29380	176281

The catalyst efficiency parameters are well correlated and suggest again that the process is highly reproducible even under FBS conditions.

In order to evaluate any potential effects induced by the presence of FC 12 on the kinetics of the process, a comparison with the values obtained for the catalyst parameters when only toluene was used is presented in Table 6.3.

Table 6.3 Activity, TON and TOF in toluene *vs* FBS conditions

Activity kg(PE)[mol(catZr)hbar]$^{-1}$		TON ($molC_2H_4/molZr$)		TOF ($molC_2H_4$ $molZr^{-1}*h^{-1}$)	
toluene	FBS	toluene	FBS	toluene	FBS
2633	2570	39171	33358	235029	200146

The values obtained for activity, TON and TOF are close and suggest that the catalyst efficiency parameters are not affected by the presence of a PFC in the system. Under our working conditions, FBS does not induce any noticeable influence on the kinetics of the coordination polymerization process.

We were also interested in investigating the effects of FBS conditions on the properties of polyethylene synthesized under such conditions. DSC was again the method used to determine the melting temperature (T_m) and polymers crystallinity (%). Table 6.4 presents the DSC results acquired for these conditions.

Table 6.4 Effects of FBS on polyethylene T_m and crystallinity

Run	T_m (°C)	Crystallinity (%)
178	137.8	34.1
179	139.7	31.7
198	138.4	28.8
202	139.1	19.3
203	137.3	30.0

The results obtained for the melting temperatures are consistent. A slight variation can be detected in the case of crystallinity, which can be explained by considering the thermodynamics of crystallization process and the thermal properties of FC 12: at high cooling rates, the entangled polymeric chains do not have the time to arrange themselves in a regular way and a structure with predominant amorphous state is thus achieved.

The melting temperature and crystallinity of polymers obtained in FBS conditions were also compared to those determined for the polymers synthesized in the presence of toluene only. These results are summarized in Table 6.5.

Table 6.5 T_m and crystallinity, toluene *vs* FBS conditions

T_m (°C)		crystallinity (%)	
toluene	FBS	toluene	FBS
138.6	137.8	43.2	34.1

The melting point data are similar for polymers obtained in toluene and those synthesized in FBS conditions. Crystallinity values are however slightly different. The slightly more amorphous state (only 34.1% crystallinity) calculated for the polymers synthesized in FBS might be determined by the influence of PFC, which does not allow the polymeric chains to arrange themselves in a regular way.

6.2 Copolymerization in FBS

Ethylene – 1-hexene copolymerization in FBS was also investigated in the presence of zirconocene dichloride (Cp_2ZrCl_2) and MAO as catalytic system. The same standard methodology, involving temperature control and catalyst activation, was used in these experiments. The comonomer and the perfluorinated solvent were injected before the ethylene monomer was introduced into the system. Concentrations of 1-hexene of 0.2, 0.5 and 0.8M were used during the copolymerization kinetic study. Copolymerization reproducibility for all comonomer concentrations was assessed in the same way as for ethylene polymerization. The results of these tests are presented in Table 6.6.

Table 6.6 Ethylene – 1-hexene copolymerization yields in FBS conditions

Run	$[C_6H_{12}]$ mol L^{-1}	Mass C_2H_4 used (g)	Mass C_6H_{12} used (g)	Theoretical polymer mass (g)	Actual polymer mass (g)	Yield (%)
239	0.2	11.07	2.82	13.89	13.86	99.8
242		10.90	2.82	13.72	13.40	97.7
238	0.5	15.45	6.30	21.75	19.80	91.0
204	0.8	7.65	10.08	17.73	8.02	45.2
206		8.17	10.08	18.25	8.22	45.0

These runs suggest that higher polymer yields are favored by a lower comonomer concentration (e.g., 0.2 mol L^{-1}). The amount of ethylene consumed in the reaction was higher when a mixture of FC 12 and toluene was used as the reaction medium (FC 12:toluene = 1:4, v/v), even though the amount of comonomer, namely 1-hexene, was constant. In FBS conditions, a comonomer effect can thus be noticed; the presence of an α-olefin enhances the ethylene polymerization rate and consumption. These results are opposite to the ones obtained when only toluene was used as reaction medium; in such conditions a negative comonomer effect was noticed. In our working conditions, the comonomer effect noticed in FBS is most likely due to the inert diluent role played by the PFC; the active complex is kept out of the polymer matrix, which positively affects the monomer diffusion limitation process.

Catalyst activity, TON and TOF were also calculated in the case of ethylene – 1-hexene copolymerization in FBS conditions. The results are presented in Table 6.7.

Table 6.7. Catalyst efficiency parameters for copolymerization in FBS conditions

Run	$[C_6H_{12}]$ mol L^{-1}	Activity kgpolymer[mol(catZr)hbar]$^{-1}$	TON (mol polymer /molZr)	TOF (mol polymer molZr^{-1}*h^{-1})
	0	2570	33358	200146
239	0.2	4582	47974	287842
242		4430	47226	283358
238	0.5	6545	66932	401593
204	0.8	2651	33172	199033
206		2717	35407	212439

Because the reaction is a copolymerization process, catalyst efficiency parameters are again affected by the presence of two monomers in the reaction medium and by their competition for the available catalytic active species. When the 1-hexene concentration is 0.2 mol L^{-1} and 0.5 mol L^{-1}, activity values are higher (4506 kgpolymer[mol(catZr)hbar]$^{-1}$ and 6545 kgpolymer[mol(catZr)hbar]$^{-1}$, respectively) than when no comonomer was present in the system. The same trend can be observed for the other two parameters, TON and TOF: higher numbers were calculated when a comonomer was present in the system than when only one monomer was involved in the process. Again, this trend can be explained by the presence of PFC, which acts as an inert diluent and helps excluding the active catalytic species from the growing polymer matrix.

Copolymers properties obtained in FBS were again evaluated using DSC. The values obtained for T_m and crystallinity are presented in Table 6.8.

Table 6.8 Effect of FBS on polyethylene T_m and crystallinity

Run	$[C_6H_{12}]$ mol L^{-1}	T_m (°C)	Crystallinity (%)
242	0.2	122.7	17.9
238	0.5	115.6	40.8
204	0.8	111.0	36.9

As seen in Table 6.8, similar values were measured for copolymers melting temperatures, whereas a higher relative proportion of amorphous structure (e.g., 17.9% crystallinity) was detected for the tests in which lower amounts of 1-hexene (e.g., 0.2 mol L^{-1}) were used. Much more crystalline structures (e.g., 40.8 and 36.9% crystallinity) were obtained for higher concentrations of comonomer. The low crystallinity values can be explained by the presence of an inert diluent in the reaction medium favors the formation short branches of 1-hexene on the main backbone polymeric chain formed mainly by ethylene units. However, this assumption has to be verified by further tests and confirmed using other techniques to determine the molecular weight M_w and M_n of the polymers (e.g., gel permeation chromatography). To confirm the assumption that the presence of an inert diluent favors the formation of short branches of a comonomer on the main backbone polymeric chain, higher M_w values should be obtained when a comonomer concentration of 0.2 mol L^{-1} was used compared to concentrations of 0.5 and 0.8 mol L^{-1}, respectively.

Another comparison was made between the values obtained for T_m and crystallinity for the copolymers synthesized in FBS with the ones measured for the copolymers obtained in the presence of toluene only. This comparison is presented in Table 6.9.

Table 6.9 T_m and crystallinity for copolymers obtained in toluene and FBS

$[C_6H_{12}]$ mol L^{-1}	T_m (°C)		Crystallinity (%)	
	toluene	FBS	toluene	FBS
0	139.1	139.5	45.5	40.9
0.2	121.9	122.7	20.8	17.9
0.5	113.6	115.6	22.6	40.8
0.8	107.0	111.0	17.1	36.9

For both types of copolymers, the melting temperature is regularly decreasing with increasing concentrations of the comonomer in the reaction medium. In terms of crystallinity, the decreasing trend is noticed only for the tests in which only toluene was used as the reaction medium. The crystallinity values strongly suggest that the copolymers obtained in the FBS conditions are more resistant and brittle than the one synthesized in the presence of toluene only. When only the hydrocarbon was used, the higher amounts of comonomer incorporated in the polymers most likely result in an increased flexibility, which decreases their processability temperature, both characteristics that are intensely exploited by polymer industry.

FT-IR was used to probe the copolymers composition, namely the amount of 1-hexene incorporated into the polymer matrix. The amount of comonomer incorporated in the matrix for the copolymers synthesized in FBS were again determined using calibration curves and A_{1380}/A_{1380} absorbance ratios. The results are presented in Table 6.10.

Table 6.10 Comonomer content in ethylene – 1-hexene copolymers in FBS conditions

Run	$[C_6H_{12}]$ mol L^{-1}	A_{1380} (cm^{-1})	A_{1370} (cm^{-1})	A_{1380}/A_{1370}	Hexene content, c_{hexene} (%)
244	0.2	0.385	0.595	0.65	1.6
245	0.5	0.441	0.529	0.83	3.0
246	0.8	0.724	1.049	0.69	2.7

As expected, the comonomer content is increasing with increasing 1-hexene concentrations. However, the results for the 1-hexene concentrations of 0.5 and 0.8 mol L^{-1} are in contradiction with the values obtained for crystallinity measured by DSC, which suggest a low relative abundance of the comonomer incorporated either in the main polymeric chain or as short branches. Further investigations using ^{13}C-NMR and gel permeation chromatography have to be performed in order to confirm these results.

Chapter 7 Conclusions

In the general context of the rapid growth of clean chemical synthetic technologies, the pathways proposed by green chemistry ensure highly efficiently chemical reactions which produce little or no waste. Within this perspective, fluorine chemistry plays an important role both in terms of catalysts and solvent replacement.

Owing to their unusual physical properties, perfluorocarbon solvents were exploited in a range of applications such as immiscible reaction medium when unstable reagents must be used. We became interested in metallocene-based polymerization of α–olefin in a fluorous biphasic system and the potential influences of this system on the coordination polymerization mechanism and physical properties of the polymers synthesized in such conditions.

The design and the set-up of a new polymerization reactor was the starting point of our study. The reactor design and set-up fulfilled some basic requirements such as the continuous feed of the reagents and monomer and resistance under a wide range of reaction conditions (e.g., high pressure and temperature). The reactor set-up was completed by a three-module controller which allowed a full control and tuning of the reaction variables (e.g., pressure, temperature, and stirring speed), as well as a data logger.

Using a very well-known and studied catalytic system, zirconocene dichloride and MAO, preliminary tests of ethylene polymerization were carried out in order to assess system performance and process stability. Even though the results of these preliminary tests showed poor reproducibility and inconsistent yields, they represented opportunities

for improving our hardware and the experimental protocol. The modifications made to our reactor setup allowed us to obtain good reproducibilities for the polymerization reactions.

The temperature and pressure variations profiles for ethylene polymerization tests carried out under standardized conditions were consistent with the results obtained in kinetic studies performed by other groups. When the polymerization time was increased, the polymer yield decreased; this trend can be explained by the homogeneous conditions of the system during the initial stages of polymerization followed by the onset of heterogeneous conditions which made the process diffusion-controlled. Catalyst activity showed the same trend, with a good correlation for the calculated values of TON and TOF. However, the duration of the polymerization process did not affect T_m and polymer crystallinity.

When the ethylene polymerization temperature was varied, TON and TOF reached maxima between 40 and 50 °C and decreased outside of this range. Polymer properties such as T_m and T_g seemed to be unaffected by reaction temperature variations. Using the Arrhenius equation, an attempt to calculate the activation energy of the process in our working conditions was made.

When ethylene – α-olefin copolymerization in toluene was investigated, the process was smoother. Higher polymer yields were obtained when lower comonomer concentrations (e.g., 0.2 mol L^{-1}) and shorter polymerization times were used. Catalyst activity, TON and TOF decreased with increasing comonomer concentration, a relationship which was evident at longer polymerization times. As expected, the presence of another comonomer decreased both T_m and polymers crystallinity. Using FT-IR as

described in the literature, an attempt was also made to evaluate the relative proportion of comonomer incorporated in the synthesized copolymers.

In the following step of our project, toluene was replaced with a fluorous biphasic system as reaction medium for ethylene polymerization and, respectively, ethylene - higher α-olefin copolymerization. Using the FBS conditions, the monomer pressure and temperature variations profiles followed a trend similar to the one recorded when only toluene was used as a reaction medium. Owing to the PFC inert diluent property however, the agglomeration of the polymer and the monomer diffusion limitation influence were minimized. In FBS conditions, catalyst efficiency parameters were also well correlated but the presence of a PFC in the reaction medium had a limited influence on the catalyst efficiency and did not have any noticeable influence on the kinetics of the coordination polymerization process.

DSC was used to evaluate the T_m and polymers crystallinity for the polymers obtained in a FBS system. For the T_m, no significant variations were noticed when compared with tests in which only toluene was used as reaction medium. The thermodynamics of the crystallization process and the thermal properties induced by the presence of FC 12 were the factors considered to explain the slight variation detected in the case of polymers crystallinity.

When ethylene – 1-hexene copolymerization reactions were performed in FBS, a negative comonomer effect was noticed most likely due to the inert diluent role played by PFC. The calculated values for catalyst efficiency parameters were lower in FBS conditions, and so they were affected by the presence of the two monomers in the reaction medium. In terms of crystallinity, a relatively higher proportion of amorphous

structure (e.g., 17.9% crystallinity) was detected for the tests in which lower amounts of 1-hexene (e.g., 0.2 mol L^{-1}) were used, whereas much higher relative proportions of crystalline structures (e.g., 40.8 and 36.9% cristallinity) were obtained for higher concentrations of comonomer. The assumption that the presence of an inert diluent in the reaction medium favors the formation of short branches on the main backbone polymeric chain formed mainly by ethylene units has to be further confirmed using other techniques (e.g., gel permeation chromatography or ^{13}C-NMR).

When copolymers crystallinity obtained in FBS were compared with those measured for the copolymers synthesized in toluene, a decreasing trend was noticed for the case when only the hydrocarbon was used as reaction medium. This fact suggests that the copolymers obtained in FBS are more resistant and brittle, so they will be more difficult to process and will require higher working temperatures.

The relative proportion of comonomer incorporated in the copolymers matrix synthesized in FBS seems to increase with increasing 1-hexene concentrations. The low relative abundance of the comonomer incorporated either in the main polymeric chain or as short branches again has to be further confirmed by other analysis methods (e.g., gel permeation chromatography or ^{13}C-NMR).

These systems show great potential provided their study and development are pursued. Future possible development directions of the work carried out in this project can be related with:

- in depth kinetics study through the addition of a thermal mass flow meter to the reactor set-up – which will allow to measure the feed rate of ethylene and thus to calculate the monomer concentration and

polymerization reaction rate. The calculated data can be confirmed with the help of gas chromatograph which will allow analyzing the gas composition in the reactor at the end of each run. A kinetic model able to fit the experimental observations can then be developed based on the collected and calculated data;

- in depth polymer characterization using a high-temperature gel permeation chromatography which would allow calculating the number-average molecular weight (M_n), weight-average molecular weight (M_w), weight-average distribution and polymer dispersity index (PDI). Also, ^{13}C nuclear magnetic resonance (NMR) would allow gathering information about short-chain branching (and thus the relative abundance of the comonomer) of the copolymer collected at the end of each run, and to calculate the triad sequence distribution.

References

1. J. R. Severn, J. C. Chadwick, R.Duchateau, N. Friederichs, *Chem. Rev.*, **2005**, 105, 4073-4147.

2. W. Kaminsky, A. Laban, *App. Catal. A: General,* **2001**, 222, 47-61.

3. P. Galli, G. Vecellio, *J. Pol. Sci.: Part A: Polym. Chem.,* **2004**, *42*, 396-415.

4. K. B. Sinclair, *Macromol. Symp.*, **2001**, *173*, 237-261.

5. G. Odian, Principles of Polymerization, forth edition, Wiley Interscience, 2004.

6. K. Ziegler, E. Holzkamp, H. Martin, H. Breil, *Angew.Chem.*, **1955**, 67, 541-547.

7. G. Natta, *Angew.Chem.*, **1956**, 68, 393-397.

8. nobelprize.org/chemistry.

9. A. E. Hamielec, J. B.P. Soares, *Prog. Polym. Sci.,* **1996**, 21, 651-706.

10. L. L. Böhm, *Macromol. Symp.*, **2001**, 173, 53-63.

11. E. J. Arlman, P.Cossee, *J. Catal.,* **1964**, 3, 99-105.

12. Encyclopedia of polymer Science and Engineering, John Wiley & Sons, New York, 1985.

13. http://alexandria.tue.nl/extra2/200510552.pdf

14. S. J. Tavener, J. H. Clark, *J. Fluorine Chem.*, **2003**, 123, 31-36.

15. D.W. Zhu, *Synthesis*, **1993**, 953-954.

16. I. T. Horvath, J.Rabai, *Science*, **1994**, 266, 72-75.

17. J. A. Gladysz, *Angew.Chem. Ind.*, **2005**, 44, 5766-5768.

18. a) L. P.Barthel-Rosa, J. A. Gladysz, *Coordination Chem. Rev.*, **1999**, 190-192, 587-605; b) J. A. Gladysz, D.P.Curran, *Tetrahedron*, **2002**, 58, 3823-3825.

19. a) T. H. Newman *Eur. Pat. Appl.*, **1990**, EP 361309 A2; b) E. Jones, J. Walker, *Ger.Offen.* **1975**, DE 2501239.

20. T. J. de Vries, R. Duchateau, M.A.G. Vorstman, J. T. F. Keurentjes, *Chem. Com.*, 2000, 263-264.

21. D. S. Breslow, N.R. Newburg, *J. Am. Chem. Soc.*, **1957**, 79, 5072-5077.

22. G. Natta, P. Pino, G. Mazzanti, U. Giannini, *J. Am. Chem. Soc.*, **1957**, 79, 2975-2980.

23. D. S. Breslow, W. P. Longs, *Liebigs Ann. Chem.*, **1957**, 463-469.

24. a) H. Sinn, W. Kaminsky, *Adv. Organomet. Chem*, **1980**, 18, 99-103; b) H. Sinn, W. Kaminsky, H. J. Vollmer, R. Woldt, *Angew. Chem. Int. Ed.*, **1980**, 19, 390-392.

25. J. A. Ewen, *J. Am. Chem. Soc.*, **1984**, 106, 6355-6359.

26. a) W. Kaminsky, *Catal. Today*, **1994**, 20, 257-262; b) H. H. Brintzinger, D. Fisher, R. Mülhaupt, B. Rieger, R. M. Waymouth, *Angew. Chem. Int. Ed. Engl.*, **1995**, 34, 1143-1147.

27. W. Kaminsky, O. Sperber, R. Werner, *Coordination Chem. Rev.*, **2006**, 250, 110-117.

28. W. Kuran, Principles of coordination polymerization, **2001**, John Wiley & Sons Ltd, Baffius Lane, Chichester, West Sussex PO 19 1UD, England, pages 103-105.

29. E. Y. X. Chen, T. J. Marks, *Chem.Rev.*, **2000**, 100, 1391-1434.

30. a) http://irs.ub.rug.nl/ppn/182206165; b) J. J. Eisch, A. M. Brownstein, E. J. Gabe, F. L. Lee, *J. Am. Chem Soc.*, **1985,** 107, 7219-7224; c) R. F. Jordan, C.S. Bajgur , R. Willett, B. Scott, *J. Am. Chem Soc.*, **1986,** 108, 7410-7417.

31. A. E. Hamielec, J. B. P. Soares, *Prog. Polym. Sci.*, **1996**, 21, 651-706.

32. a) P. Cossee, *J. Catal.*, **1964**, 3, 80-87; b) E. J. Arlman, P.Cossee, *J. Catal.*, **1964**, 3, 99-104.

33. I. T. Horvath, *Acc. Chem. Res.*, **1998**, 31, 641-650.

34. T. E. Nowlin, Y.V.Kissin, K. P. Wagner, *J. Pol. Sci. Part A, Pol. Chem.*, **1988,** 26, 755-764.

35. A. H. Tullo, *Chem. Eng. News*, **2003**, 81, 26-27.

36. a) J. C. W. Chien, B. Wang, *J. Pol. Sci., Part A, Pol. Chem.*, **1988**, 26, 3089-3102; b) T. Tsutsui, N. Kashiwa, *Polym. Com.*, **1988**, 29, 180-183; c) J. C. W. Chien, *J. Pol. Sci., Part A, Pol. Chem.*, **1990**, 28, 15-38; d) M. Vela Estrada, A.E. Hamielec, *Polymer*, **1994**, 35, 808-818; e) B. Rieger, C. Janiak, *Die Angewandte Makr. Chem.*, **1994**, 215, 35-46; f) C. Janiak, U. Versteeg, K. C. H. Lange, R. Weimann, E. Hahn, *J. Org. Chem.*, **1995**, 501, 219 – 234; g) G. P. Belov, H. R. Gyulumyan, I. M. Khrapova, V. P. Maryin, N. N. Korneev, *J. Mol. Cat. A. Chem.*, **1997**, 115, 155-161; h) A. R. Siedle, W. M. Lamana, R. A. Newmark, J. N. Schroepfer, *J. Mol. Cat. A. Chem.*, **1998**, 128, 257-271; i) J. Huang, G. L. Rempel, *Polym. Reaction Eng.*, **1997**, 5, 125-139; j) M. M. Marques, A. R. Dias, C. Costa, F. Lemos, F. R. Ribeiro, *Polym. Intr.*, **1997**, 43, 77-85; k) M. M. Marques, A. R.

Dias, C. Costa, F. Lemos, F. R. Ribeiro, *Polym. Intr.*, **1997**, 43, 86-96; l) P. A. Charpentier, A. E. Hamielec, S. Zhu, *Polymer*, **1998**, 39, 6501-6511; m) K. Thorshaug, J. A. Stovneng, E. Rytter, M. Ystenes, *Macromol.*, **1998**, 31, 7149 – 7165; n) E. Ochoteco, M. Vecino, M. Montes, J. C. de la Cal, *Chem. Eng. Scie.*, **2001**, 56, 4169-4179 ; o) K. Tannous, J. B. P. Soares, *Macromol. Chem. Phys.*, **2002**, 203, 1895-1905; p) F. Song, R. D. Cannon, M. Bochmann, *J. Am. Chem. Soc.*, **2003**, 125, 7641-7653; q) K. P. Bryliakov, N. V. Semikolenova, D. Y. Yudaev, V. A. Zakharov, H. H. Brintzinger, M. Ystenes, E. Rytter, E., P. Talsi, *J. Org. Chem.*, **2003**, 683, 92-102; r) L. A. Nekhaeva, G. N. Bondarenko, V. M. Frolov, *Kinetics and Catalysis*, **2003**, 44, 692-699; s) J. J. Eisch, P. O. Otieno, J. N. Gitua, A. A. Adeosun, *Eur. J. Org. Chem.*, **2005**, 4364 -4371.

37. a) J. M. Vela Estrada, A. E. Hamielec, *Polymer*, **1994**, 35, 808-818; b) G. C. Han-Adebekum, J. A. Debling, W. H. Ray, *J. Appl. Polym. Sci.*, **1997**, 64, 373-382 ; c) P. A. Charpentier, A. E. Hamielec, S. Zhu, *Polymer*, **1998**, 39, 6501-6511 ; d) E. Ochoteco, M. Vecino, M. Montes, J. C. de la Cal, *Chem. Eng. Sci.*, **2001**, 56, 4169-4179 ; e) K. Tannous, J. B. P. Soares, *Macromol. Chem. Phys.*, **2002**, 203, 1895 – 1905.

38. Parr Instruments Co. specific literature for series 5100 low pressure reactors.

39. L. D'Agnillo, J. B. P. Soares, A. Pendilis, *J. Polym. Chem. Sci., Part A: Polym. Chem.*, **1998**, 36, 831-840.

40. J. Wu, Q. Pan, G. L. Rempel, *J. Appl. Pol. Sci.*,**2005**, 96, 645-649.

41. B. Rieger, C. Janiak, *Angew. Makr. Chem.*, **1994**, 215, 35-46.

42. J. Huang, G. L. Rempel, *Polym. Reaction Eng.*, **1997**, 5, 125-139.

43. W. Kaminsky, O. Sperber, R. Werner, *Coord. Chem. Rev.*, **2006**, 250, 110-117.

44. G. V. Loukova, A. I. Mikhailov, A. E. Shilov, *Kin. and Catal.*, **2002**, 43, 799-800.

45. J. C. W. Chien, T. Nozaki, *J. Pol. Sci. Part A*, **1993**, 31, 227-237.

46. J. Koivumäki, J. Seppälä, *Macromol.*, **1993**, 26, 5535-5538.

47. P. Lo Nostro, L. Scalise, P. Baglioni, *J. Chem. Eng. Data,* **2005**, 50, 1148-1152.

48. H. C. Cho, H. L. Strauss, R. C. Snyder, *J. Phys. Chem.*, **1996**, 96, 5290-5295.

49. a) J. G. Riess, *Tetrahedron*, **2002**, 58, 4113-4131. b) M. P. Krafft, *Adv. Drug Delivery Rev.*, **2001**, 47, 209-228.

50. S. J. Tavener, J. H. Clark, *J. Fluorine Chem.*, **2003**, 123, 31-36.

51. L. P. Barthel-Rosa, J. A. Gladysz, *Coord. Chem. Rev.*, **1999**, 190-192, 587-605.